



저작자표시-비영리-변경금지 2.0 대한민국

이용자는 아래의 조건을 따르는 경우에 한하여 자유롭게

- 이 저작물을 복제, 배포, 전송, 전시, 공연 및 방송할 수 있습니다.

다음과 같은 조건을 따라야 합니다:



저작자표시. 귀하는 원저작자를 표시하여야 합니다.



비영리. 귀하는 이 저작물을 영리 목적으로 이용할 수 없습니다.



변경금지. 귀하는 이 저작물을 개작, 변형 또는 가공할 수 없습니다.

- 귀하는, 이 저작물의 재이용이나 배포의 경우, 이 저작물에 적용된 이용허락조건을 명확하게 나타내어야 합니다.
- 저작권자로부터 별도의 허가를 받으면 이러한 조건들은 적용되지 않습니다.

저작권법에 따른 이용자의 권리는 위의 내용에 의하여 영향을 받지 않습니다.

이것은 [이용허락규약\(Legal Code\)](#)을 이해하기 쉽게 요약한 것입니다.

[Disclaimer](#)

농학석사 학위논문

Spatial distribution analysis of
Black-legged Kittiwakes and Northern Fulmars
in Svalbard coastal cliffs
using remotely piloted aircraft system

원격조종항공기시스템을 활용한 스발바르 해안절벽의
세가락갈매기 및 풀머갈매기에 대한 공간 분포 분석

2020 년 8 월

서울대학교 대학원
산림과학부 산림환경학전공
박 미 진

Spatial distribution analysis of
Black-legged Kittiwakes and Northern Fulmars
in Svalbard coastal cliffs
using remotely piloted aircraft system

원격조종항공기시스템을 활용한 스발바르 해안절벽의
세가락갈매기 및 풀머갈매기에 대한 공간 분포 분석

지도 교수 임 상 준

이 논문을 농학석사 학위논문으로 제출함
2020 년 8 월

서울대학교 대학원
산림과학부 산림환경학전공
박 미 진

박미진의 농학석사 학위논문을 인준함
2020 년 7 월

위 원 장	_____	(인)
부위원장	_____	(인)
위 원	_____	(인)

Abstract

It is crucial to estimate the exact number of individuals and to understand population dynamics in conservation biology. Although seabirds play an important role as top predators in marine ecosystems, low accessibility often limits effective monitoring on colonial cliff-nesting seabirds in coastal cliffs. In this study, the remotely piloted aircraft system (RPAS) was applied to investigate colonial cliff-nesting seabirds, especially Black-legged Kittiwakes (*Rissa tridactyla*) and Northern Fulmars (*Fulmarus glacialis*), in the extreme environment of the Norwegian Svalbard archipelago in the Arctic Ocean.

During the breeding season in 2018 and 2019, RGB (red, green, and blue) and thermal images of coastal cliffs were acquired from RPAS to construct three-dimensional models of study sites. These models were then used to count total seabirds and analyze spatial distribution of kittiwakes and fulmars. The models composed of RPAS-driven RGB and thermal images were compared with the photos taken by a researcher on the ground, where visible or hidden areas on the observer points were determined by viewshed analysis of GIS (Geographic Information System) software. Thermal images were processed according to temperature values and pixel sizes, and examples of composite uses with RGB images were also suggested. The density, which was defined as the mean value of the number of neighboring adult kittiwakes within a radius of 0.8m distance, was calculated, and the relationship between the density and each colony size was examined. Also, the fulmar chicks were observed to investigate the occupation of similar nest site in Steinflåstupet where the surveys were conducted over two years in the same way.

The counting result of the Irgensfjellet colony suggested that on average 1.6 times more kittiwakes were detected in the RPAS-driven RGB image model than in merged photos taken by a ground observer. On the other hand, the counts were not significantly different among models at Krykkjefjellet, which had a higher proportion of visible areas than Irgensfjellet, because topography was accessible enough to observe. This study also confirmed the complementary potential of

thermal images in seabird monitoring associated with RGB images to discover cryptic individuals. In addition, semi-automated counting of seabirds was possible when the range of the temperature values and pixel sizes were properly adjusted and sorted. RPAS data to estimate the densities of adult kittiwakes demonstrated that the traditional observation may commit errors, which may lead to overestimate the kittiwake density than that of three-dimensional models. Same nest sites were occupied over two years in that seven fulmar chicks detected in 2019 were all settled in the already observed nest site of 2018.

In conclusion, RPAS may act as a considerable tool for monitoring of cliff-nesting seabirds when RGB and thermal camera were combined. An analysis on the density and spatial distribution would be extendedly applied on other cliff-nesting seabirds. Like fulmars with high nest site preferences, nest site changes over the years could be recorded by RPAS with respect to long-term monitoring.

Keyword: RPAS, Svalbard seabird, coastal cliff, cliff-nesting, colonial breeding, Black-legged Kittiwake, Northern Fulmar

Student Number: 2018-21328

Table of contents

Abstract	i
Table of contents	iii
List of tables	v
List of figures	vi
Chapter 1. Introduction	1
1.1. Study background	1
1.2. Purpose of research	2
Chapter 2. Literature review	4
2.1. Seabirds in the Svalbard Archipelago	4
2.2. Cliff-nesting adaptation	6
2.3. Colonial breeding	6
2.4. Precedent monitoring method	7
Chapter 3. Materials and methods	9
3.1. Study sites and period	9
3.2. Image acquisition	11
3.3. Model construction and manual counting	14
3.4. Seabird identification through RGB and thermal images ..	15
3.5. Comparison among colonies and inter-annual change	16
Chapter 4. Results	18
4.1. Image acquisition and model construction	18
4.2. Reliable counts through post processing	20
4.3. Seabird identification and survey results	23
4.4. Density measurements	31

Chapter 5. Discussion	36
5.1. Applicability of RPAS on monitoring seabirds	36
5.2. Usage of thermal images	37
5.3. Density measurements	38
5.4. Long-term monitoring	39
 Chapter 6. Conclusions	 40
 References	 41
 Appendix	 47
 Abstract in Korean	 69

List of tables

Table 1. Precedent studies of colonial cliff-nesting seabirds	8
Table 2. Population sizes of the Black-legged Kittiwake (<i>Rissa tridactyla</i>) near Ny-Ålesund in the summer seasons	28
Table 3. Population sizes of the Northern Fulmar (<i>Fulmarus glacialis</i>) near Ny-Ålesund in the summer seasons	29
Table 4. Population sizes of other seabird species near Ny-Ålesund in this study	30
Table 5. The comparison of inter-annual nest site changes in Steinflåstupet.....	37

List of figures

Figure 1. The map of the Svalbard Archipelago and six study sites of Svalbard coastal cliffs.	11
Figure 2. Overall flight scheme to a targeted colony.	14
Figure 3. Two ways to calculate the density of adult kittiwakes within a small colony in Krykkjefjellet.	17
Figure 4. Site images during the flight, taken on the coastal cliff. ..	21
Figure 5. Box-whisker plots of manual counts with different images in Krykkjefjellet and (B).	23
Figure 6. The calculation of viewsheds in (A) Krykkjefjellet (visible area: 34.3% of DEM raster grid) and (B) Irgensfjellet (visible area: 17.6% of DEM raster grid).	24
Figure 7. Examples of complementary use of thermal images in (A) Irgensfjellet and (B) Kiærfjellet.	26
Figure 8. Examples of semi-automated counts with thermal images in Ossian Sarsfjellet (A) subcolony D and (B) subcolony A.	28
Figure 9. The map of observed species observed by ground-based and RPAS-based survey in the six study sites.	29
Figure 10. The scatter plot of calculated densities and size of colony.	34

Figure 11. (A) A histogram of the distribution of the number of neighbors in captured view (2D) and exported markers (3D) and (B) suggested reason of the difference. 35

Figure 12. Examples of image sets exhibiting inter-annual nest sites in Steinflåstupet. 37

Chapter 1. Introduction

1.1. Study background

Keeping track of the exact number of individuals is crucial to understand the population dynamics of wild animal and to establish a conservation plan (Morrison 1994). As avian species occupy highly different types of habitat from forest to ocean, birds were used to evaluate the integrity of ecosystem (Jaspers et al. 2007). In the Arctic marine ecosystem, seabirds have been used as an indicator to reflect the marine food availability (Cairns 1988) or contaminants like plastic debris (Mallory 2008) and to predict the increase or decrease in sea-ice coverage (Mallory et al. 2006).

However, researchers have had difficulties in surveying birds because of low accessibility to their extreme habitats (Rush et al. 2018). Colonial seabirds inhabiting cliffs are one of the difficult groups to monitor because seabirds distribute vertically along the irregular cliff surface, and the approach to seabirds is perilous due to the possibility of erosion (Bird 1994). In spite of dangerousness, researchers have estimated the densities (Harris et al. 1997; Massaro et al. 2001; Birkhead 1977) and measured the topographical features manually (Kildaw 1999; Squibb and Hunt Jr 1983). The problem still remains even for indirect approaches; cliff is a characterful topography in that conventional ground mapping could less reflect the horizontal ruggedness. Restricted observations may result in biases for the estimates of seabird abundance (Buckland et al. 2008). Colonial breeding is another obstacle because the survey results would vary depending on the reliability of monitoring technique (Hutchinson 1980) and demand labor-intensive works.

In many recent instances, those traditional monitoring techniques would be replaced by remotely piloted aircraft system (RPAS) to some extent (Gonzalez et al. 2016). The diverse sizes and designs of aircraft were developed (Anderson and Gaston 2013; Mackenzie 2012a, 2012b), and the declining cost of aircrafts lead to the explosive increase of utilizing RPAS on such ecological studies (Weissensteiner et al. 2015).

In bird monitoring, RPAS has been applied over the last decade (Sardà-Palomera et al. 2012; Chabot and Bird 2012). RPAS is in multifaceted use of monitoring a large colony of the Common Tern (*Sterna hirundo*) (Chabot et al. 2015) and detecting cryptic nests of the Field Sparrow (*Spizella pusilla*) (Scholten et al. 2019) and the Northern Lapwing (*Vanellus nanellus*) (Israel and Reinhard 2017). In other previous studies, penguins were considered as the suitable model species to estimate the population size because the nests of penguin family (Spheniscidae) are relatively prominent. Almost 4,300 breeding individuals of Adélie (*Pygoscelis adeliae*) and Chinstrap Penguins (*Pygoscelis antarcticus*) were surveyed in King George Island, but the limitation was that aerial images taken at a height of 550m above sea level were unsatisfactory to distinguish two species (Korczak-Abshire et al. 2019). In case of a flight altitude of 30m, the colony dominated by a thousand Gentoo Penguins (*Pygoscelis papua*) was individually discriminated (Ratcliffe et al. 2015). The survey conducted by Goebel et al. (2015) showed the photograph counts were quite reliable, 2.4% to 3.9% less estimated in total, compared to ground counts.

By adopting RPAS, fine-spatial analysis would also be accomplished in cliff-nesting seabirds. The coastal cliffs have been frequently surveyed by civil engineers and geographers in the perspective of risk management (Jaud et al. 2019; Fazio et al. 2019). RPAS combined with high-resolution camera would help to reduce variances with off-site error checking (Hodgson et al. 2016). One empirical research presented that the counts in images were more approximate to actual figures of the replica seabird colonies than in the study site (Hodgson et al. 2018).

1.2. Purpose of research

In this study, I endeavored to survey Arctic seabird species, which have both colonial breeding and cliff-nesting behavior. Because Arctic seabirds are the main consumers in the Arctic ecosystem, they have been rigorously monitored in the Norwegian Svalbard Archipelago on a regular basis under the SEAPOP (SEAbird POPulations) programme since 2005 (Anker-Nilssen et al. 2008). However, the key

parameters of seabird population such as population change, annual adult survival, and reproductive performance have been generally derived only from a few plot counts (Anker-Nilssen et al. 2019). Thus, I aimed to operate RPAS to successfully acquire the image of seabirds and coastal cliffs as a newly adapted monitoring technique. With the increased accessibility, three-dimensional (3D) model could be constructed from obtained images and then used in the identification of seabirds, quantitative analysis of spatial density, and inter-annual comparison of nest sites.

Chapter 2. Literature review

2.1. Seabirds in the Svalbard Archipelago

The Svalbard Archipelago ranges from 74°N to 81°N and 10°E to 35°E in the Arctic Ocean. As Svalbard shows a typical High Arctic climate, many parts of the land are covered with glaciers. Spitsbergen, Nordaustlandet, Edgerøya, and Barentsrøya are the four main islands of Svalbard, but they are different in the vegetation cover. The central and northern Spitsbergen where the long and wide fjords established have the relatively low percentage of glaciers and the high percentage of non-vegetated areas and shadows instead (Johansen et al. 2012).

Ny-Ålesund (78.92342°N, 11.93196°E) is located on the north part of Brøggerhalvøya, which is situated on the western coast of Spitsbergen, and abuts the shore of Kongsfjorden. Kongsfjorden primarily carries Northern Shrimps (*Pandalus borealis*), Polar Cods (*Boreogadus saida*), Atlantic cods (*Gadus morhua*), and Greenland Halibuts (*Reinhardtius hippoglossoides*), which support marine mammals and seabirds (Hop et al. 2002). In particular, the West Spitsbergen Current from Atlantic Water and the East Spitsbergen Current from Arctic Water influence the sea ice extent around Svalbard and ultimately the whole food webs (Descamps et al. 2017; Svendsen et al. 2002).

The occupation history of a colony could be proposed by analyzing the sediments (Liguang et al. 2004), and seabirds in Ny-Ålesund were known to colonize more than 9,400 years ago after the deglaciation of Kongsfjorden (Yuan et al. 2010). Nine species were reported to go breed in summer in the marine ecosystem of Kongsfjorden: Common Eider (*Somateria mollissima*), Little Auk (*Alle alle*), Black Guillemot (*Cepphus grille*), Atlantic Puffin (*Fratercula arctica*), Thick-billed Murre (*Uria lomvia*), Northern Fulmar (*Fulmarus glacialis*), Black-legged Kittiwake (*Rissa tridactyla*), Glaucous Gull (*Larus hyperboreus*), and Arctic Tern (*Sterna paradisaea*) (Hop et al. 2002).

The seabirds near Ny-Ålesund can be classified according to foraging strategies; guillemots and puffins are pursuit divers, eiders are benthic feeders, and gull-like species are surface feeders (Hop et al. 2002; Dahl et al. 2003). Because the diet represents the ecological niche they occupy, seabirds were used to reveal the food web structure (Iverson et al. 2007). Black-legged Kittiwakes in Svalbard were used as a bioindicator of Atlantification in the Arctic Ocean (Vihtakari et al. 2018). Other species such as the Thick-billed Murre, Little Auk, Black Guillemot, Northern Fulmar, and Glaucous Gull were also suggested as bioindicators from stable isotope analysis which reflect diet and trophic position (Hobson and Bond 2012).

Abundance, species-specific properties, and residency patterns were investigated to estimate the consumed biomass by seabirds (Hop et al. 2002). A total of 4,000 pairs of eiders, 1,000 pairs of Little Auks, 100 pairs of Black Guillemots, 50 pairs of puffins, 1,700 pairs of Thick-billed Murres, 1,000 pairs of fulmars, 5,200 pairs of kittiwakes, 100 pairs of Glaucous Gulls, and 1,500 pairs of terns were estimated (Hop et al. 2002). The more exact estimates could be produced by the more precise population data.

The population sizes of each seabird were available at SEAPOP data portal (<http://www2.nina.no/Seapop/>), and the detailed last observation records of seabird near Ny-Ålesund in summer could be downloaded under the geographical selection of Kongsfjorden municipality (Appendix 1). The main coastal cliffs were in Blomstrandhalvøya, Brøggerfjellet, Kiærstranda, Krykkjefjellet, Ossian Sarsfjellet, and Stuphallet. In Blomstrandhalvøya or Blomstrandhamna except for Bird Sanctuary, Black-legged Kittiwake and Thick-billed Murre were the dominant species; 908 apparently occupied nests (AONs) of kittiwakes and 239 pairs of Thick-billed Murres were observed in 2011. Approximate 300 pairs of puffins were mainly counted in Brøggerfjellet in 1973. In Kiærstranda or Kiærfjellet, approximate 700 AONs of fulmars were counted in 1973, and 400 pairs of puffins in 1983. 806 pairs of kittiwakes were detected in Krykkjefjellet in 1992, and Little Auks also colonized in 1985. Ossian Sarsfjellet was the largest habitat containing 1,936 AONs of kittiwakes and 1,358 individuals of Thick-billed Murres in 2011. Fulmar was dominant in Stuphallet or Steinflåstupet in 2011.

2.2. Cliff-nesting adaptation

Recent phylogenetic approach suggested that cliff-nesting is likely to appear later in the evolutionary history (Fang et al. 2018). Nevertheless, distinctive behavioral adaption to cliff-nesting is observed in some avian taxa such as the kittiwake (Cullen 1957), Swallow-tailed Gull (*Creagrus furcatus*) (Hailman 1965), Black Noddy (*Anous tenuirostris*) (Cullen and Ashmole 1963; Ashmole 1962) and the Northern Gannet (*Sula bassana*) (Danchin and Nelson 1991; Nelson 1965).

Cullen was one of the first researchers who reported cliff-nesting adaptation in Black-legged Kittiwakes. Kittiwakes are known to nest on narrow ledges by elaborate nest-building technique with mud and fibrous materials, so that deeply cupped nests would contribute to the lower predation on kittiwake eggs and chicks (Cullen 1957).

The Northern Fulmar and Thick-billed Murre are also cliff-nesting species, but these two seabirds do not build conspicuous nests unlike kittiwakes (Squibb and Hunt Jr 1983). The observation in Alaska elucidated the spatial segregation between the kittiwakes and the fulmars, in that the fulmars locate higher cliffs with vegetation (Fisher 1966). However, the kittiwakes are usually more competitive than the fulmars to deprive of breeding sites (Coulson and Horobin 1972). Such competition would give rise to displacement in order not to overlap similar nest sites even within relative species (Kildaw 1999).

2.3. Colonial breeding

Coulson (2002) stated seabirds that live and breed close would have at least long-term advantages, and many researchers have suggested various hypotheses on the coloniality. Some seabirds may be forced to colonially breed owing to the lack of adequate nest sites (Rowan 1952), but the main advantage of large colonies would be the reduced predation risk (Coulson 2002). The fortunate young would have a

higher chance of avoiding predators with synchronized breeding, resulting in a higher breeding success (Hailman 1964; Darling 1938).

Almost all seabird species have evolved to breed colonially (Danchin and Wagner 1997), and the colony size may vary (Brown et al. 1990). Northern Fulmars can be more gregarious than 100,000 nests, Thick-billed Murres up to 800,000 nests, and Atlantic Puffins up to 148,000 nests (Brown et al. 1990; Birkhead and Nettleship 1985; Fisher 1952).

2.4. Precedent monitoring method

The fundamental way to monitor seabirds was to individually mark them with metal or colored plastic leg-ring, so that the continuous monitoring of a colony could be conducted (Aebischer and Coulson 1990). The nest density was produced based on a virtual surface or simply classified into qualitative description in the precedent studies (Table 1). Harris et al. (1997) and Massaro et al. (2001) respectively measured the incubating birds and nests within three body lengths, designated as unit area. Other topographical features regarding nest site characteristics such as ledge width, length, or slope were measured point by point because the ledges were demonstrated to be one factor of nest site preferences among different species (Kildaw 1999; Squibb and Hunt Jr 1983). The density along with broad and narrow ledge was emphasized because those factors combined with the density and topographical features were closely relevant to breeding success (Birkhead 1977).

Table 1. Precedent studies of colonial cliff-nesting seabirds

Reference	Species	Study area	Measuring the (nest) density
Birkhead (1977)	Common Guillemot (<i>Uria aalge</i>)	Skomer Island, Wales, United Kingdom (51°40'N, 05°15'W)	<ul style="list-style-type: none"> • Dense = broad ledge, > 10 birds/m² • Medium = narrow ledge • Sparse = broad ledge, < 3 birds/m²
Harris et al. (1997)	Common Guillemot	Isle of May, Scotland, United Kingdom (56°11.1'N, 2°33.5'W)	<ul style="list-style-type: none"> • Neighbors = the number of incubating birds touching the bird incubating at the site (ca. 1 m²) • Density = the number of incubating birds within three body lengths of the site
Massaro et al. (2001)	Black-legged Kittiwake	Gull Island, Newfoundland and Labrador, Canada (47°16'N, 52°46'W)	<ul style="list-style-type: none"> • n = the number of nests within a radius of three kittiwake body lengths (ca. 0.8m) • High = > 4 nests/1.8m² • Medium = 3 nests/1.8m² • Low = 1 - 2 nests/1.8m²

Chapter 3. Materials and methods

3.1. Study sites and period

From the late July to early August of 2018 and 2019, I visited the coastal cliffs near Ny-Ålesund in the Svalbard Archipelago, Norway (Fig 1). Based on the published population data, I observed six seabird colonies with various sizes: Krykkjefjellet (78.89632°N, 12.19484°E), Ossian Sarsfjellet (78.93280°N, 12.44011°E), Irgensfjellet (78.99408°N, 12.11681°E), Steinflåstupet (78.95809°N, 11.60749°E), Kiærfjellet (78.90680°N, 11.50234°E), and Simlestupet (78.99408°N, 12.11681°E) (Fig 1). The biggest colony was in the Ossian Sars Nature Reserve (Ossian Sarsfjellet), and the smallest ones were in Steinflåstupet and Kiærfjellet.

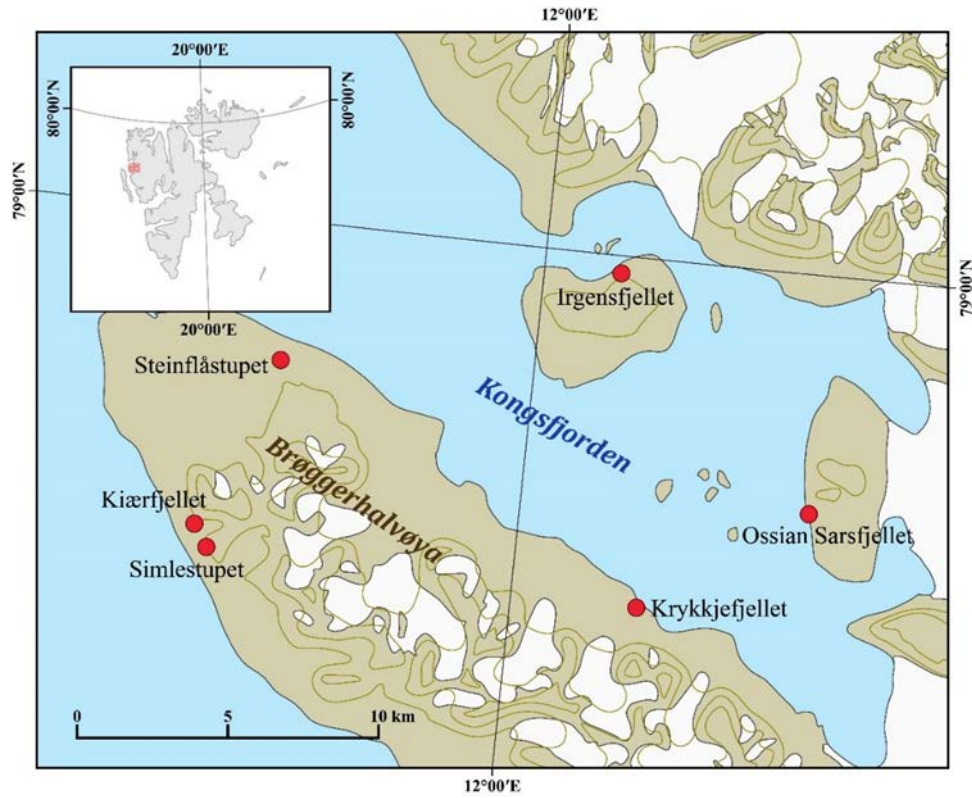


Figure 1. The map of the Svalbard Archipelago and six study sites of Svalbard coastal cliffs. Study sites are located in Brøggerhalvøya or surrounded by the shore of Kongsfjorden.

3.2. Image acquisition

3.2.2. RPAS equipment and flight conditions

I deployed a customized commercial aircraft model (DAYA-550 Alien Carbon Fiber Folding Quadcopter Frame Kit; DAYA, China) powered with four motors (MN3508 KV700; T-Motor, Jiangxi, China) and 12-inch propellers. Flight controller (Pixhawk 2; PX4 AutoPilot, Zürich, Switzerland) was used within radio telemetry system (Transceiver Telemetry Radio V3 433MHz; Holybro, Guangdong, China). A long-range radio system (FrSky R9 & R9M 900MHz; FrSky Electronic Co., Jiangsu, China) and a controller (FrSky Taranis Q K7; FrSky Electronic Co., Jiangsu, China) were selected to meet the working frequency band of EU version. A distance sensor measurable up to 120m (SF11/C LIDAR Range Sensor; Lightware Visual Engineering, Budapest, Hungary) was compatible with the flight controller. Two types of camera were attached under the quadcopter: visible light (SONY DSC-RX0 4800x3200; Sony Corporation, Tokyo, Japan) and thermal imaging infrared camera (FLIR Vue Pro R 640x512; FLIR Systems, Oregon, USA). The weight of aircraft with battery was approximately 1,500g and the other detachable payload was about 500g. Maximum flight time was 20 minutes per a lithium polymer battery (PT-B4200N-UKP45; Poly-Tronics, China).

The six coastal cliffs were investigated by an aircraft under a speed of 5m/s when the wind is light and the sunshine is not too bright (Appendix 2). A series of RGB (red, green, and blue) and thermal images were programmed to snap: one RGB image per two seconds and one thermal image per second, considering their camera angles. In addition, I included geographical identification metadata while piloting the aircraft. However, not all images were geotagged because it was almost impossible to plan the automatic flights due to obstacles or unexpected wind.

All kinds of disturbance could not be excluded, but the aircraft was skillfully maneuvered in order not to disturb the targeted birds following the protocol (Ditmer et al. 2015; Hodgson and Koh 2016; Rush et al. 2018; Kellenberger et al. 2018). I first designed to approach a small colony in the margin of each cliff and recorded the response of seabirds toward flying aircraft. Taking pictures of the main colony was

continued only if they did not express any aggressive behavior. While inspecting the distance sensor, the aircraft was operated as close to the cliff as possible. In general, the aircraft kept the distance of 50m and then zigzaggedly approached closer to the distance of 20m (Fig 2). I was greatly watchful to any sudden shift in the surroundings and ready to abort the flight at any time as a countermeasure.

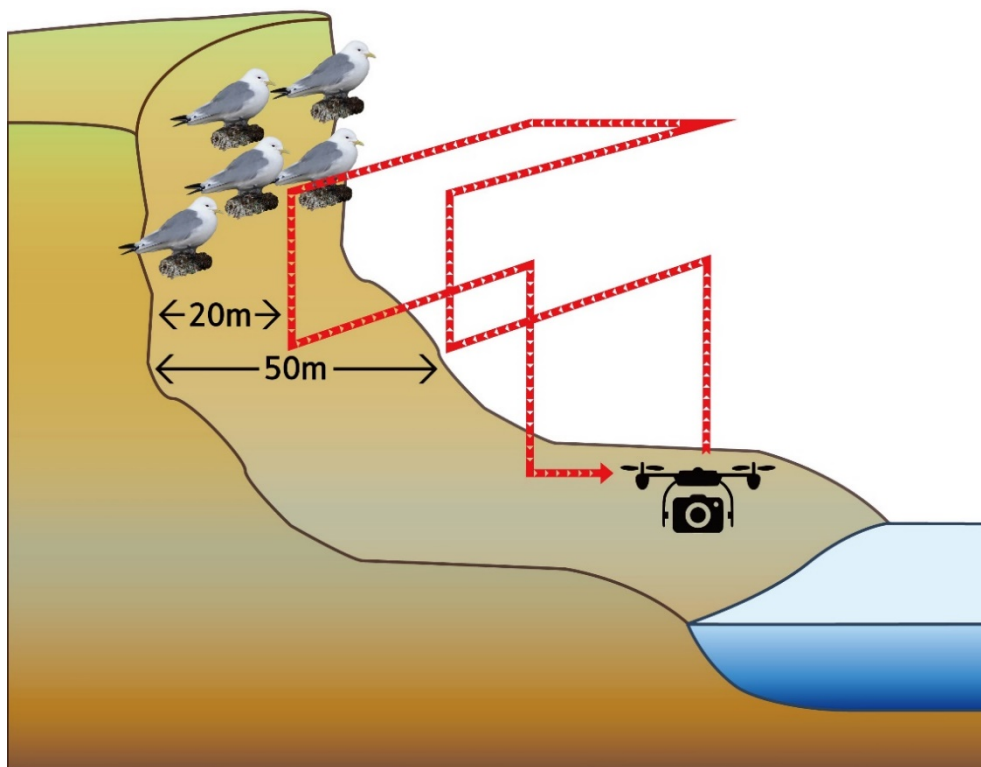


Figure 2. Overall flight scheme to a targeted colony. The aircraft was launched on the ground and slowly approached to colonies from a distance 50m to 20m and even closer.

3.2.2. Ethical statements

This research was conducted under permissions from the Governor of Svalbard and other Norwegian authorities, complying the guideline stated by Kings Bay. I was notified from the Governor of Svalbard that I should abide by general rules under the Svalbard Environmental Protection Act (ref. 1091212-2). I declared the type of RPAS (RO1) to the Norwegian Civil Aviation Authority (CAA), which had to be light-weight under 2.5kg and slowly piloted under 120 meters (NO.RPAS.5720). I obtained the temporary permission from Norwegian Communications Authority (Nkom) for use of radio frequencies ranging from 433.05 to 434.79MHz, available within 20 km from Ny-Ålesund (ref. 1903705-4-533). I consulted with the Norwegian National Security Authority (NSM) and Norwegian Mapping Authority (NMA) and registered the airborne sensor usage. Regarding aviation safety, the flight activities were insured by liability and property coverage. I signed a coordination agreement with Ny-Ålesund Airport and daily informed the planned flight schedule prior to use. All procedures were reported to Ny-Ålesund Science Managers Committee (NySMAC) project information and discussion (PID) forum, and the overview could be simply accessed in Research in Svalbard (RiS) database under RiS-ID 11249.

3.3. Model construction and manual counting

3.3.1. Three-dimensional model construction

Various software has made it simple to construct 3D models of coastal cliffs by Structure-from-Motion (SfM) photogrammetry (Forsmo et al. 2019). A software, Agisoft Metashape 1.6.2 (LLC Agisoft, St. Petersburg, Russia), was used to overlap the RPAS-driven RGB and thermal images. All RGB images were taken with 4800x3200 pixels, and thermal images were 640x512 pixels in a lump during flights. I followed the four steps to generate as other studies achieved (Burns et al. 2015; Ventura et al. 2018): (i) align photos, (ii) build dense cloud, (iii) build mesh, and (iv) build texture. If the images were geotagged, they were automatically aligned; otherwise, I manually designated the coordinates and elevation of several noticeable terrain features, which were obtained from the digital maps in TopoSvalbard (<https://toposvalbard.npolar.no/>) of the Norwegian Polar Institute.

3.3.2. Different methods for manual counting

I compared the seabird monitoring method between traditional ground photographic counting and RPAS-based model counting. I took RGB photos (SONY DSC-RX10M4 5472x3648; Sony Corporation, Tokyo, Japan) on the ground while the aircraft was piloted, and I merged these ground-taken photos with Adobe Photoshop CS6 (Adobe Inc., California, USA) to represent the observer's view. The seabird figurations in the constructed models were pinpointed, utilizing "Add Marker" function in Metashape. To confirm these enumerated counts, I tested if the reliable figures could be consistently derived from other people. The two subsets of Krykkjefjellet and Irgensfjellet images were presented to several independent researchers. Each subset comprised three image groups: (i) the merged photos taken by a researcher on the ground, (ii) the constructed model from RPAS-driven RGB images, and (iii) the constructed model from RPAS-driven thermal images.

The manual counting was conducted, and the counts were recorded. The counts were plotted with ggplot2 package (Wickham 2011) in R 3.6.2. (R Core Team, Vienna, Austria) and statistically tested among three image groups in each subset.

First, Shapiro-Wilk normality test was used to test the univariate normality in each group. Second, if the data meet normality, one-way analysis of variance (ANOVA) followed by all pairwise multiple comparison procedures (Tukey test) could be processed to exclude the effect of individual researcher. Otherwise, non-parametric alternatives of Kruskal-Wallis test and Tukey test would be gone through if normality was not satisfied.

3.3.3. Viewshed analysis

To support the result from different monitoring methods above, the viewsheds from an observer point were analyzed. The two RPAS-driven RGB image models and markers of Krykkjefjellet and Irgensfjellet were exported as digital elevation models (DEM) of 1cm pixel resolution from Metashape. The models were imported in ArcGIS Pro 2.5 (Esri, California, USA), and the markers of seabird were plotted as points in the same way. The seabirds were hypothesized as the spheres within the radius of 0.1m, so that the spheres were created by “Buffer 3D”. DEMs were analyzed by “Viewshed” function with the designated observer point, and the buffered points (spheres) containing the viewshed value were counted with QGIS 3.10.4 “Zonal statistics”.

3.4. Seabird identification through RGB and thermal images

Thermal images, simultaneously taken with RGB images, were selected and converted with FLIR ResearchIR software (FLIR Systems, Oregon, USA). Contours were constructed with ArcGIS “Contour List” and “Feature to polygon” function, and tiny (< 3 pixel sizes) or extremely large contour polygons (> 40 – 100 pixel sizes depending on the distance) which did not indicate the size of seabirds were removed. Processed thermal images were compared with RGB images to validate the presence of seabirds. Same method as described above was used for semi-automated counts.

3.5. Comparison among colonies and inter-annual change

3.5.1. Density calculations

I compared the four densities of the kittiwake, which was a dominant species at Krykkjefjellet, Ossian Sarsfjellet, Irgensfjellet, and Simlestupet. In this study, I would count the neighbors as the number of adult kittiwakes within a spherical radius of three kittiwake body lengths (ca. 0.8m) modified from Massaro et al. (2001) (Fig 3A). I also defined the density as the mean value of the neighbors within each colony.

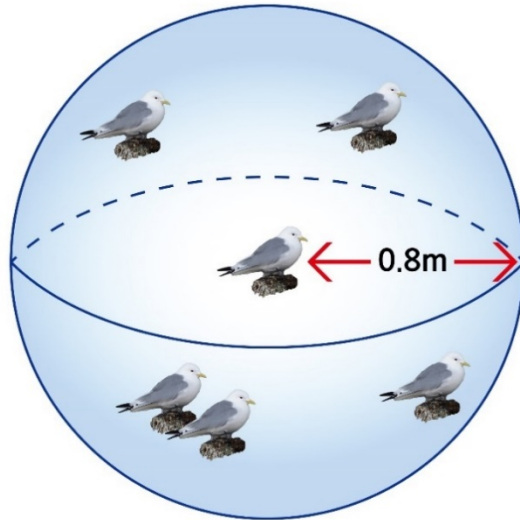
I exported the estimated coordinates and altitude of each marker from the models to three-dimensionally analyze the distance between markers. The initial coordination system of markers was transformed from WGS 84 (EPSG 4326) into ETRS 89/UTM zone 33N (EPSG 25833) with Pyproj package (<https://github.com/pyproj4/pyproj>) in Python 3.7.6 (Python Software Foundation, Delaware, USA). Distances between markers were calculated, and neighboring markers within 0.8m were recorded with python NumPy package (Oliphant 2007). The calculated densities were adopted to all 3D habitat models and plotted with regression model to show a tendency between the density and colony size by python matplotlib (Hunter 2007) and statsmodels package (Seabold and Perktold 2010).

To compare the result following the traditional method of Massaro et al. (2001), I captured the 3D model of Krykkjefjellet subcolony to simulate field survey (Fig 3B). The number of adult kittiwakes within a radius of three kittiwake body lengths was counted on the captured view. The densities calculated by “exported markers” and from “captured view” were displayed as histogram and compared by the Chi-square test with python matplotlib and SciPy package (Virtanen et al. 2020).

3.5.2. Nest site detections

A Northern Fulmar colony in Steinflåstupet was monitored in consecutive two years during the summer in 2018 and 2019. I pinpointed the location of fulmar chicks as marker in Metashape to check if fulmars had occupied similar nest site over the years. The detected nest sites were named, and ground-taken RGB images were paired to figure out the re-occupation of each nest site.

(A)



(B)



Figure 3. Two ways to calculate the density of adult kittiwakes within a small colony in Krykkjefjellet. (A) The distance between each marker representing the location of adult kittiwakes was three-dimensionally calculated, and markers within a spherical radius of 0.8m were counted; (B) adult kittiwakes were manually counted within the radius of three kittiwake body lengths on the simulated view of a ground observer.

Chapter 4. Results

4.1. Image acquisition and model construction

No noticeable movement of kittiwakes was observed during the flight of RPAS, and the number of circling kittiwakes was relatively constant shown in the site image (Fig 4A). However, some individual kittiwakes continuously tried to chase away the aerial predator, the Glaucous Gull, from the nest sites with the aggressive behavior (Fig 4B).

Total 35 flights were successfully launched to cover six coastal cliffs (Appendix 2), and 17 3D habitat models containing RGB images were constructed (Appendix 3). These models were mosaicked from the photos taken with the same camera on the same day. Some cliffs had subcolonies which were at least 20m apart from the main colony, and the subcolonies in Irgensfjellet were called right and left according to the relative location. Ossian Sarsfjellet stretched 600m, so this study site was not able to be covered by one flight. Therefore, disconnected colonies were arbitrarily named: subcolony A, B, C, and D.

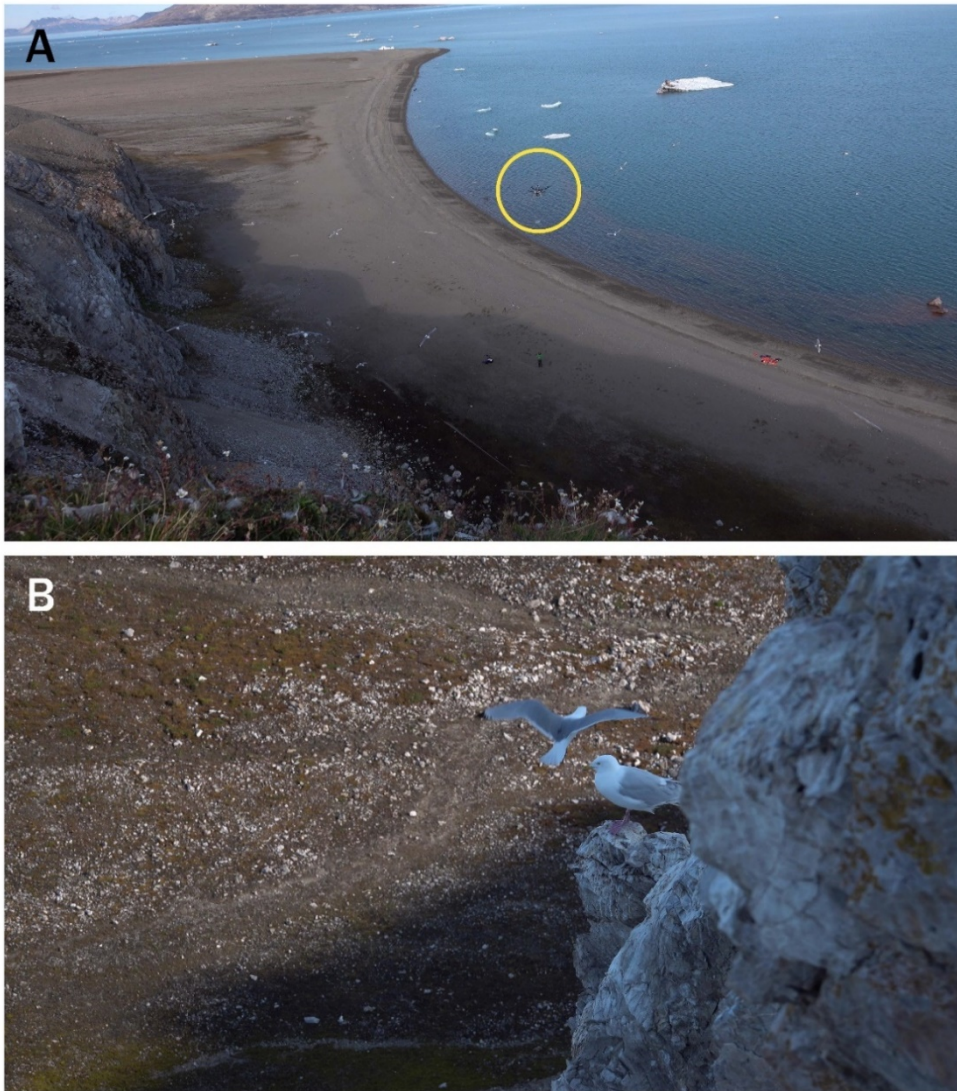


Figure 4. Site images during the flight, taken on the coastal cliff. (A) Kittiwakes did not show any behavioral difference while a remotely piloted aircraft took a series of images, but (B) kittiwakes showed aggressive behavior toward a Glaucous Gull.

4.2. Reliable counts through post processing

4.2.1. Comparison between ground-taken RGB images and constructed models

Seven independent researchers manually counted kittiwakes in Krykkjefjellet and Irgensfjellet images. The counts in each group did not meet the univariate normality, so the Kruskal-Wallis test was used and followed by all pairwise multiple comparison procedures using the Tukey test ($p < 0.05$). The results were presented with box-whisker plots (Fig 5). Counts from three different methods were not significantly different at Krykkjefjellet ($H = 5.388$ $df = 2$, $p = 0.068$), while there was a significant difference in count data among methods at Irgensfjellet ($H = 16.179$, $df = 2$, $p = <0.001$). The following pairwise multiple comparison on ranks indicated that all three count methods produced different results ($p < 0.05$) at Irgensfjellet.

4.2.2. Viewshed analysis

Under ArcGIS viewshed function, the binary viewsheds of Krykkjefjellet and Irgensfjellet were created from each observer point (Fig 6): visible raster grid reclassified into '1', and invisible into '0'. The visible area in Krykkjefjellet occupied 34.3% of DEM raster grid, and 49 out of 73 adult kittiwake buffered points touched or included the visible area (Fig 6A). Viewshed in Irgensfjellet was about 17.6% of the raster grid, and 63 out of 103 points were counted in visible area (Fig 6B).

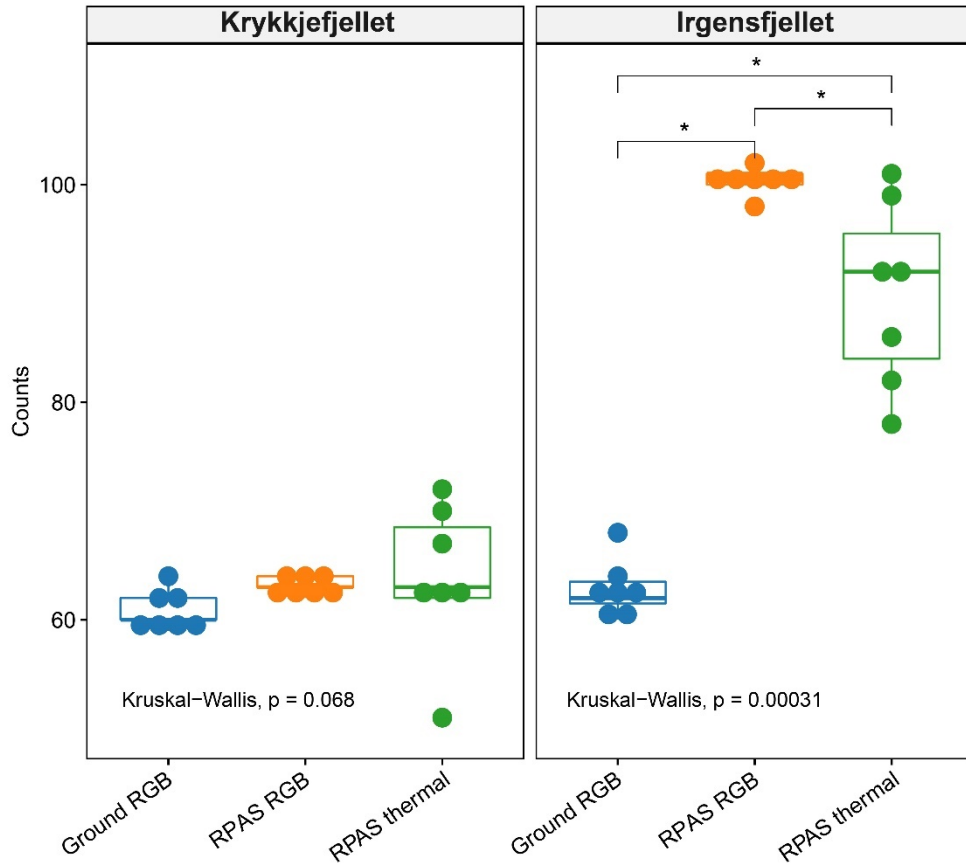


Figure 5. Box-whisker plots of manual counts with different images in Krykkjefjellet and Irgensfjellet. The Kruskal-Wallis test was significant ($p < 0.001$) at Irgensfjellet, which manual counts were statistically different by image sets, supported by the Tukey test. Asterisk indicates a significant difference ($p < 0.05$).

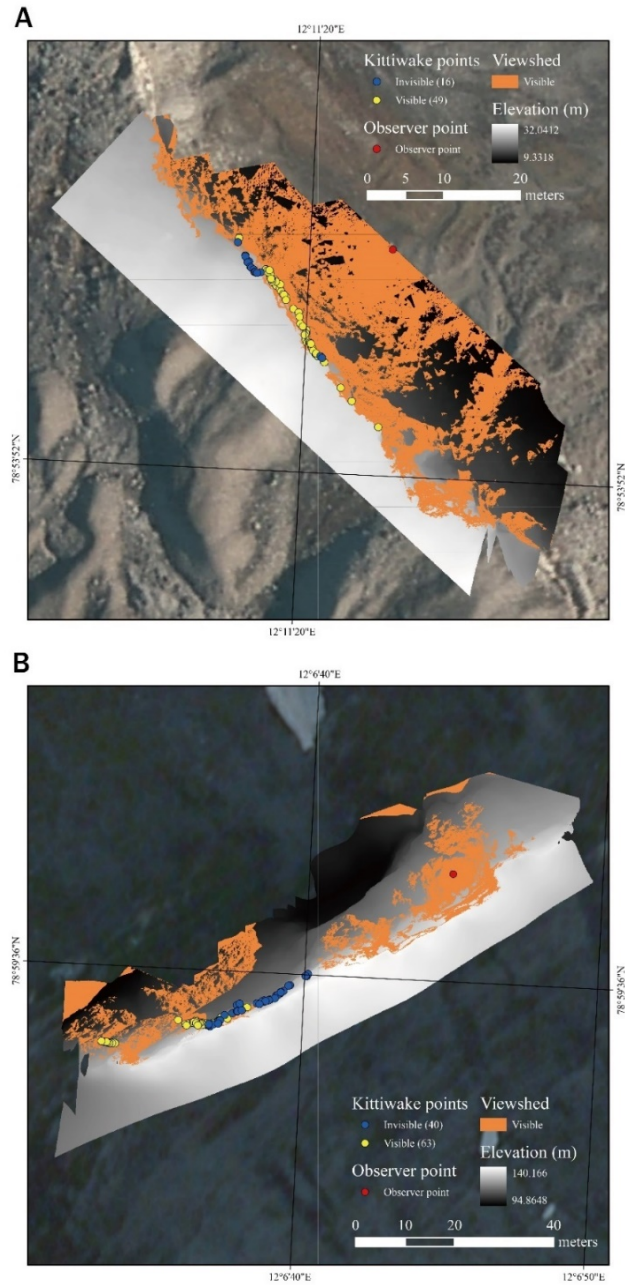


Figure 6. The calculation of viewsheds in (A) Krykkjefjellet (visible area: 34.3% of DEM raster grid) and (B) Irgensfjellet (visible area: 17.6% of DEM raster grid). (A) 16 out of 73 and (B) 40 out of 103 kittiwake points were situated on the invisible viewshed.

4.3. Seabird identification and survey results

4.3.1. Complementary use of thermal images

Thermal images were helpful in detecting cryptic fulmars. Fig 7 showed that fulmars are somewhat indistinguishable in RGB images because of the similarity of color between fulmar chicks and the bedrock. The first thermal image taken in Irgensfjellet presented 12 isothermal polygons higher than 8°C, and these 12 polygons were matched with the position of fulmars in the first RGB image (Fig 7A). However, not all fulmars were correctly discovered; one adult was omitted as below 8°C isothermal line, another adult contained two separated polygons, and the other case was one gathered polygon of adjacent adult and chick. The second thermal image taken in Kiærfjellet also presented 13 isothermal polygons higher than 12°C, fitted to the second RGB image (Fig 7B). Same problem occurred; 7 fulmars were missing with 12°C contour polygons.

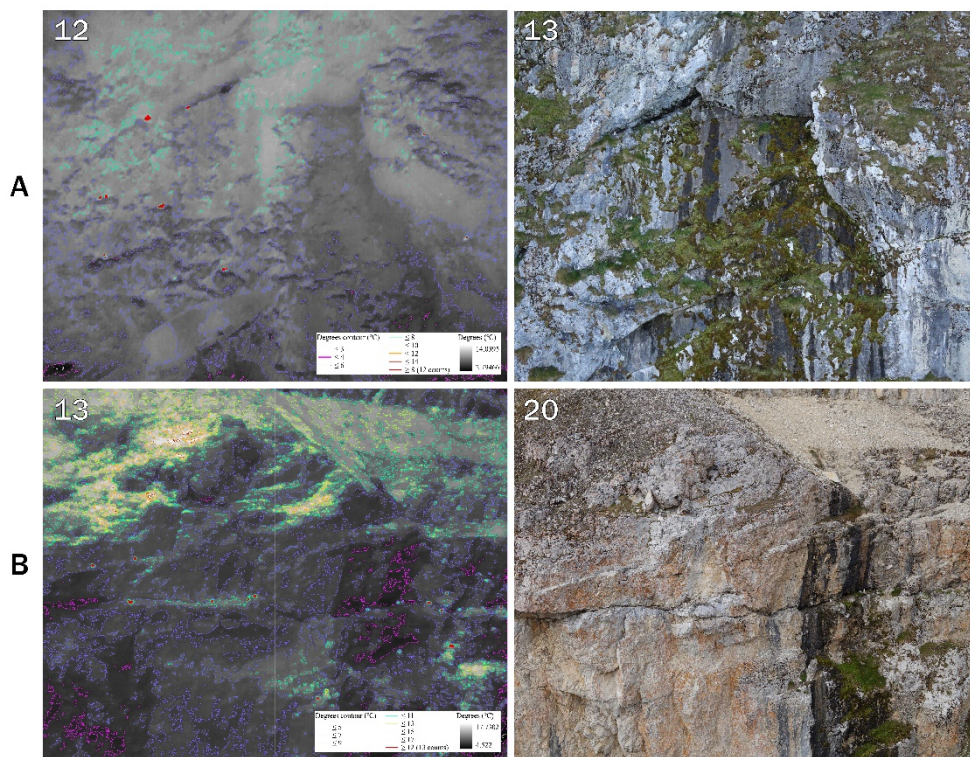


Figure 7. Examples of complementary use of thermal images in (A) Irgensfjellet and (B) Kiærfjellet. (A) 12 and 13, (B) 13 and 20 fulmars were respectively detected in a thermal and RGB image of the same angle.

4.3.2. Semi-automated counts in thermal images

The first set of RGB and thermal image was taken 8m apart from the cliff of Ossian Sarsfjellet D subcolony (Fig 8A). The thermal image provided 42 semi-automated counts, and it was soundly matched with the RGB image which was clearly taken. However, the actual number of adult kittiwakes was 37, implying the overestimated result in this case. It seemed that several contour polygons in thermal images were actually part of one kittiwake. Because eyes and feet are not feathered and display highest temperature, the contour setting higher than 16°C would exclude feathered body whose temperature was closer to the surroundings. Also, some pairs were just next to each other and made the bigger merged polygons.

The second set of RGB and thermal image was taken 13m apart in subcolony A that kittiwakes were almost in half size of the first RGB image (Fig 8B). A total of 58 out of 72 semi-automated counts in thermal image were validated to be actual adult kittiwake in RGB image. Meanwhile, 87 adult kittiwakes were observed in the RGB image, as well as five Thick-billed Murres and a Glaucous Gull chick. Thick-billed Murres and Glaucous Gulls were also included as contour polygons in the thermal image, implying that distinguishing kittiwakes from other species was not enough with two filters.

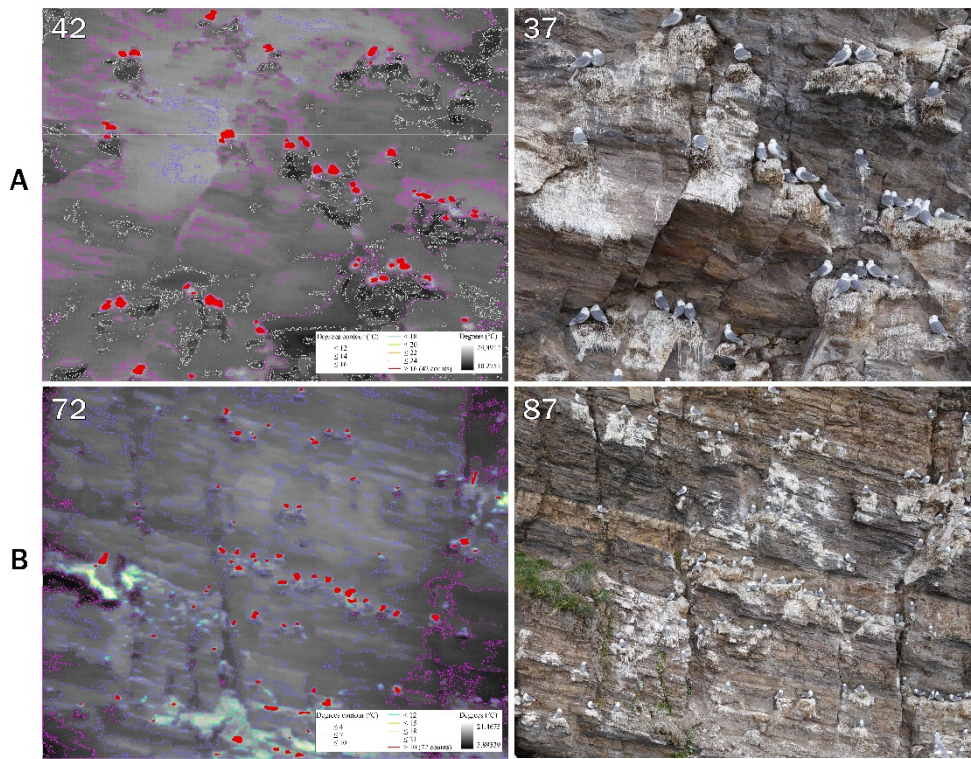


Figure 8. Examples of semi-automated counts with thermal images in Ossian Sarsfjellet (A) subcolony D and (B) subcolony A. (A) 42 and 37, (B) 72 and 87 kittiwakes were respectively detected in a thermal and RGB image of the same angle.

4.3.3. Overall survey results

The seabirds were marked individually with the 3D habitat models, and six species were detected (Fig 9). Krykkjefjellet, Ossian Sarsfjellet, Irgensfjellet, and Simlestupet were dominated by Black-legged Kittiwakes, and this dominance was also recorded in the past SEAPOP data (Table 2). On the other hand, Northern Fulmars and Atlantic Puffins mainly consisted of the colonies in Steinflåstupet and Kiærfjellet, and SEAPOP data supported this community composition (Table 3). The population sizes of the Atlantic Puffin, Black Guillemot, Glaucous Gull, and the Thick-billed Murre were listed in each study site (Table 4).

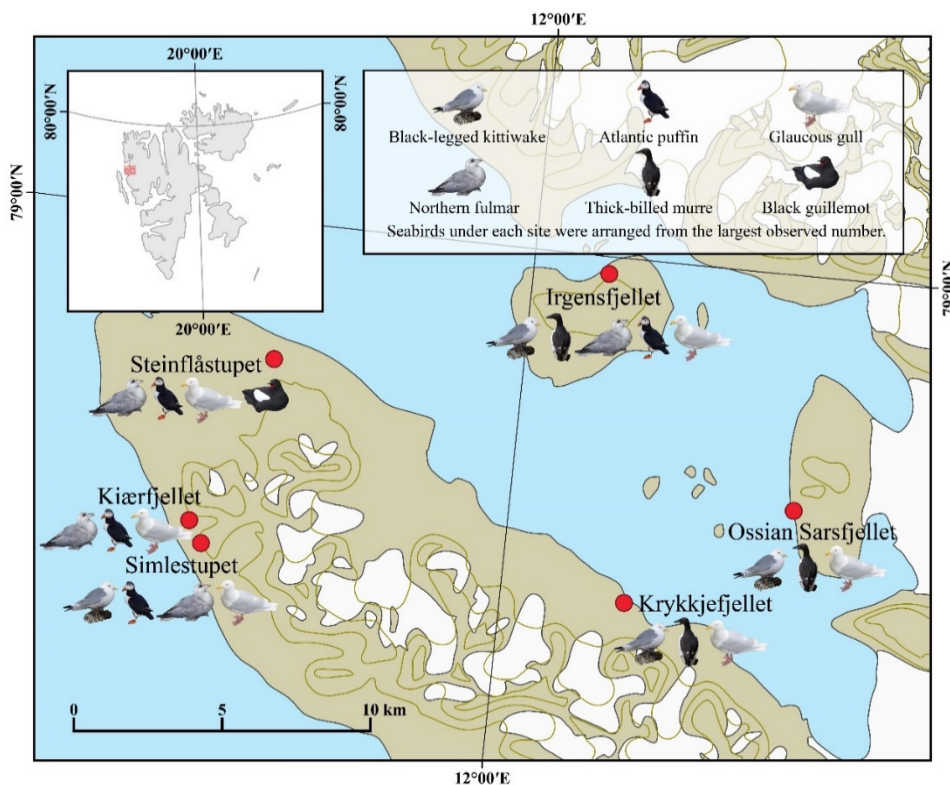


Figure 9. The map of seabird species observed by ground-based and RPAS-based survey in the six study sites.

Table 2. Population sizes of the Black-legged Kittiwake (*Rissa tridactyla*) near Ny-Ålesund in the summer seasons

Study site	Detailed location	Period	Counts	Count unit*	Reference
Krykkjefjellet	Tyskleir	13.07.1992	154	Pair	SEAPOP
	Franskleir	14.07.1992	652	Pair	SEAPOP
	Main	25.07.2019	563	Individual	This study
	Sub	26.07.2019	79	Individual	This study
	Main	04.08.2019	652	Individual	This study
	Sub	04.08.2019	73	Individual	This study
Irgensfjellet	Blomstrandhamna 3	24.07.1981	194	Pair	SEAPOP
	Blomstrandhamna 1	23.06.2011	908	AON	SEAPOP
	Main	30.07.2019	786	Individual	This study
	Main	02.08.2019	836	Individual	This study
	Right	02.08.2019	124	Individual	This study
	Left	02.08.2019	137	Individual	This study
Ossian Sarsfjellet	Ossian Sarsfjellet	18.07.2011	1936	AON	SEAPOP
	C	27.07.2019	1860	Individual	This study
	D	27.07.2019	323	Individual	This study
	C	29.07.2019	1879	Individual	This study
	D	29.07.2019	357	Individual	This study
	A	30.07.2019	1446	Individual	This study
	B	30.07.2019	1469	Individual	This study
Simlestupet		31.07.2019	1070	Individual	This study

* The abbreviation “AON” means apparently occupied nest / nest site

Table 3. Population sizes of the Northern Fulmar (*Fulmarus glacialis*) near Ny-Ålesund in the summer seasons

Study site	Detailed location	Period	Counts	Count unit*	Reference
Kiærfjellet	Kiærstranda	21.07.1973	700	AON	SEAPOP
		31.07.2019	28	Individual	This study
Irgensfjellet	Blomstrandhamna 3	24.07.1981	50	AON	SEAPOP
	Blomstrandhamna 1	23.06.2011	10	AON	SEAPOP
	Blomstrandhalvøya SW	15.07.2011	32	AON	SEAPOP
	Main	30.07.2019	14	Individual	This study
	Main	02.08.2019	27	Individual	This study
	Right	02.08.2019	27	Individual	This study
Steinflåstupet	Stuphallet	15.07.2011	127	AON	SEAPOP
		04.08.2018	38	Individual	This study
		24.07.2019	57	Individual	This study
Simlestupet		31.07.2019	14	Individual	This study

* The abbreviation “AON” means apparently occupied nest / nest site

Table 4. Population sizes of other seabird species near Ny-Ålesund in this study

Study site	Colony	Species	Period	Counts*
Krykkjefjellet	Main	Glaucous Gull	25.07.2019	1
		Thick-billed Murre		43
	Sub	Glaucous Gull	26.07.2019	2
	Main	Thick-billed Murre	04.08.2019	9
Ossian Sarsfjellet	C	Glaucous Gull	27.07.2019	20
		Thick-billed Murre		127
	D	Thick-billed Murre	27.07.2019	91
	C	Black Guillemot	29.07.2019	1
		Glaucous Gull		7
		Thick-billed Murre		130
	D	Thick-billed Murre	29.07.2019	87
	A	Glaucous Gull	30.07.2019	2
		Thick-billed Murre		318
	B	Glaucous Gull	30.07.2019	1
		Thick-billed Murre		316
Irgensfjellet	Main	Glaucous Gull	30.07.2019	2
		Thick-billed Murre		1
		Atlantic Puffin		9
	Main	Atlantic Puffin	02.08.2019	3
	Right	Thick-billed Murre	02.08.2019	16
Steinflåstupet		Atlantic Puffin	04.08.2018	19
		Atlantic Puffin	24.07.2019	18
		Glaucous Gull		2
Kiærfjellet		Atlantic Puffin	31.07.2019	16
		Glaucous Gull		2
Simlestupet		Atlantic Puffin	31.07.2019	20
		Glaucous Gull		13

* All were counted individually

4.4. Density measurements

4.4.1. Calculated densities

The densities calculated from 15 kittiwake-dominant habitat models were plotted with the x-axis of size of colony in a log scale with a linear regression line of ordinary least squares method [$Y = 0.514 (p = 0.0507) \times X + 1.138 (p = 0.101)$, $R^2 = 0.263$, $p = 0.507$, $n = 15$] (Fig 10). The density was inclinable to increase in larger colony size; the highest density was 3.04, calculated in subcolony C of Ossian Sarsfjellet containing 1879 individuals, and the lowest density was 1.54 in right subcolony of Krykkjefjellet with 73 individuals.

Histogram on the number of neighbors was plotted to compare two different counting methods (Fig 11A). From the simulated perspective or “captured view”, the number of kittiwakes which do not have any neighbor was 15, but 22 in spherical analysis by “exported markers” (Fig 11A). This difference was statistically proved according to the Chi-square test ($\chi^2 = 166.962$, $df = 1$, $p = 0.0137$). To explain this difference, a plausible situation was proposed as observation errors from the captured view may occur because of a similar effect of projection (Fig 11B). In other words, the difference would be narrowed down when the cliff wall is almost vertically flat, so a real 3D distance between each marker was similar to a projected distance despite fine-spatial surface ruggedness.

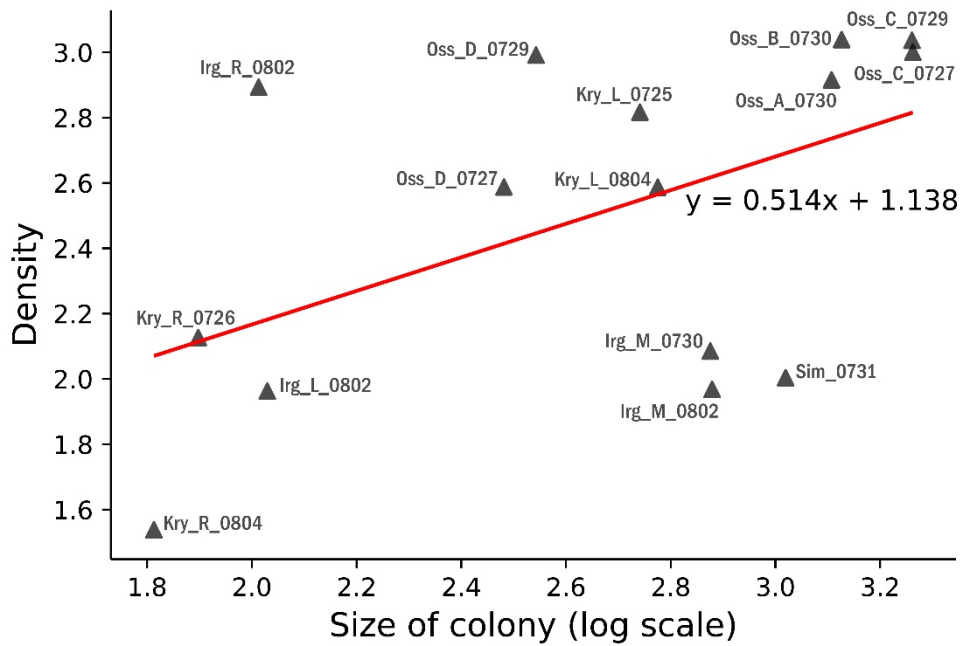
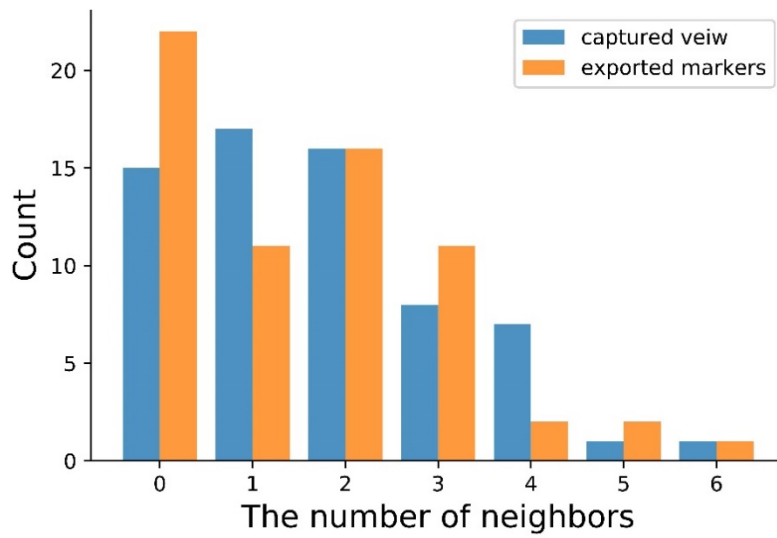


Figure 10. The scatter plot of calculated densities and size of colony. A linear regression line of ordinary least squares method [$Y = 0.514$ ($p = 0.0507$) $\times X + 1.138$ ($p = 0.101$), $R^2 = 0.263$, $p = 0.507$, $n = 15$] was also illustrated.

(A)



(B)

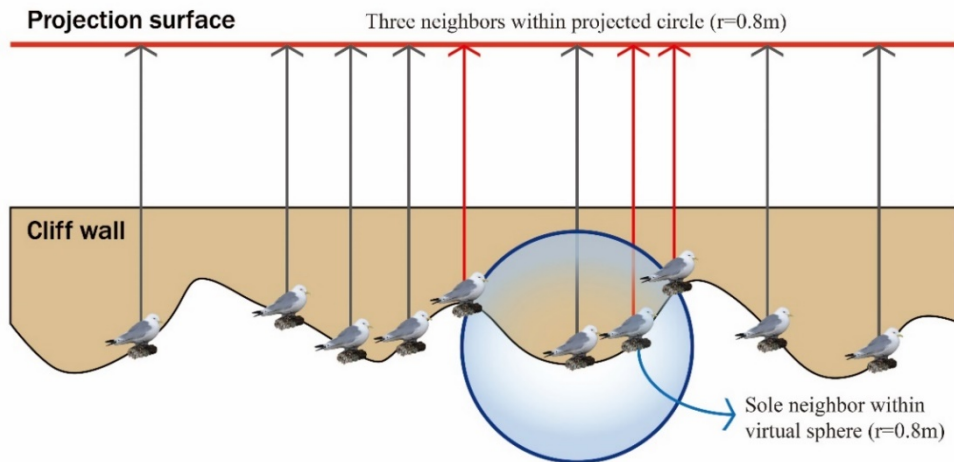


Figure 11. (A) A histogram of the distribution of the number of neighbors in captured view (2D) and exported markers (3D) and (B) suggested reason of the difference.

4.4.2. Inter-annual nest site monitoring

The 12 fulmar chicks were located on RPAS-driven RGB image models of Steinflåstupet in 2018, and 7 in 2019. Fulmar chicks were settled in the horizontal crack of bedrock (Fig 12). The nest sites were matched with the compared sets of ground-taken RGB images whose resolution was high enough to distinguish cryptic fulmar chicks from grayish bedrock (Table 5; Fig 12).

Table 5. The comparison of inter-annual nest site changes in Steinflåstupet

	2018	2019
Nest site A	○	○
Nest site B	○	
Nest site C	○	○
Nest site D	○	
Nest site E	○	○
Nest site F	○	
Nest site G	○	
Nest site H	○	
Nest site I	○	○
Nest site J	○	○
Nest site K	○	○
Nest site L	○	○



Figure 12. Examples of image sets exhibiting inter-annual nest sites in Steinflåstupet.

Chapter 5. Discussion

5.1. Applicability of RPAS on monitoring seabirds

The results showed that RPAS may successfully produce sufficient RGB images for 3D habitat model construction through SfM photogrammetry (Appendix 3). The least 68 images could cover the left colony in Irgensfjellet, which horizontally stretched about 70m (Appendix 3-17), and the most 613 images were aligned to build the main colony of 127m high Irgensfjellet (Appendix 3-14). The processing time relied on the number of images, so that the quality should be economically adjusted from the lowest to medium.

Coastal cliffs would be especially dangerous to approach, but RPAS made it practicable to observe colonial cliff-nesting seabirds. One concern was the wind speed because cliff-nesting seabirds may have advantage of strong wind (Gilchrist and Gaston 1997). An unexpected gust would lead to a catastrophic event such as a crash of an aircraft against a cliff wall or even seabirds. Therefore, the operator should check a weather forecast in advance and an onsite wind speed prior to the launch.

3D habitat models constructed by SfM photogrammetry produced reliable and more counts especially in remote and steep cliff (Fig 4; Fig 5). The observer stood at approachable location at 75m far away from the colony in Irgensfjellet, but only 20m away in Krykkjefjellet. The visual field was restricted by topographical obstacles in Irgensfjellet, so almost 40% of kittiwakes were not detected by ground-taken RGB images. The viewshed analysis also supported this result that the percentages of visible area '1' in binary classification (Wheatley and Gillings 2000) was almost double in Krykkjefjellet than in Irgensfjellet (Fig 6B).

3D habitat models provided available platform for a total census of colonial seabirds (Rush et al. 2018). The colony size in Ossian Sarsfjellet was approximate 5,000 with an individual adult count unit, and 16 to 30 minutes of flight time were required to cover the subcolony C and D (Appendix 2). It is important to select proper

type and size of aircraft considering the targeted colony size, and a fixed-wing aircraft would be beneficial in possessing longer survey time (Ratcliffe et al. 2015).

The exact number of seabirds were counted through 3D habitat models, but the existing survey results were sometimes based on the count unit of AON or pair, not in individual. This mismatch generated from different count units has been dealt with the use of correction factor k , which is breeding pairs divided by total count of birds (Harris et al. 2015; Harris 1989; Birkhead and Nettleship 1980; Birkhead 1978). The practicable value of k was estimated as 0.67 for the Common Guillemot (*Uria aalge*) in Britain and Ireland even if the correction factor varied in colonies and yearly fluctuated (Harris et al. 2015).

Simply multiplying this value to Thick-billed Murres, a species in the same genus of the Common Guillemot, in Ossian Sarsfjellet, approximate 570 pairs would be estimated as 850 individuals were observed (Table 4). The value could be adjusted to 0.61 which was used in mainland Norway (Barrett et al. 2006; Bakken 1986). Similarly, the composite nest to adult ratio of the Black-legged Kittiwake was 0.68 (Kildaw 1998), so the 3200 pairs would be estimated in Ossian Sarsfjellet, which are larger population estimates than the recent census in 2011 (Table 2). On the other hand, estimated 400 pairs of kittiwakes would be shrunk in size in the main colony of Krykkjefjellet, compared to 652 pairs recorded in 1992 (Table 2).

5.2. Usage of thermal images

As thermal images were maximized with RGB images, an exclusive usage of thermal images would be inadequate. The main reason in this study would be because the thermal camera had far fewer pixels (640x512) than the visible light camera (4800x3200). Although a high-resolution thermal camera at an equivalent level of visible light camera was used, it would not be such cost-effective (Gade and Moeslund 2014). In this respect, the counting results in RPAS-driven thermal image model expressed the larger variance than mosaicked image or RPAS-driven RGB image model, representing that even skilled researchers would be confused (Fig 5).

Moreover, other background hotspots or false-positive shapes such as warm feet and eyes (McCafferty 2013) would still mislead the count results.

When processing thermal images to display complementary use and semi-automated count, I only adopted two filters through isothermal line and size of pixels for processing thermal images. The two filters were implemental in quickly discovering cryptic seabirds, which contributed to precise monitoring. Because the surface temperature of chicks was generally higher than adults, the brightest hotspots in thermal images were used to represent the presence of chicks, serving as a good reference.

However, there were also various limitations. It was restrictive to distinguish other species in thermal images, so that RGB images were needed for validation. For example, the Thick-billed Murre had a lengthwise elongated shape, so the shapes in thermal images were separately recognized in naked eyes. Moreover, some false-negative polygons were revealed as the heated bedrock or vegetated covers, which may distort the results. Nevertheless, many image processing algorithms were recently developed to find local maximum temperature (Lhoest et al. 2015; Burke et al. 2019; Shao et al. 2020) or automated peak picking (Klukowski et al. 2018), improving the detection rate.

5.3. Density measurements

The 3D density calculated with the exported markers in this study. One of the advantages of calculating 3D density was to reflect an actual 3D distance. Precedent density measurement slightly tended to include additional kittiwake due to projection error even though both methods showed the subcolony in Krykkjefjellet had a low density (Fig 11). Moreover, the observer's interpretation on which kittiwake was included or not within the radius of three body length would be excluded in calculating 3D density.

The exported markers enabled to briefly calculate 3D density even in large colony with python script. Density monitoring in large colonies would be labor-

intensive to count each neighbor in the field. Counting and recording each neighbor might be confused by moving seabirds. However, the 3D density was quantitatively measured by one criterion and made it possible to grasp the relationship between abundance and density with sufficiently pre-identified markers (Fig 10).

Finally, 3D density estimates could compare the overall densities among the kittiwake colonies (Fig 11). In other words, an intra-specific comparison among the kittiwake colonies was only considered in this study, but the densities of other species such as the Thick-billed Murre could also be calculated under proper criteria. In addition, the distribution pattern with a factor of elevation would be suggested as fulmars occupied the higher cliff (Fisher 1952), so the spatial segregation could be detected.

5.4. Long-term monitoring

3D habitat models presented the possibility of inter-annual monitoring of fine-spatially detected nest site in Steinflåstupet. Fulmars sometimes occupy the same nests which were used in the previous years (Coulson and Horobin 1972). In this study, the entire seven fulmar chicks detected in 2019 settled in the same nest sites in 2018 (Table 5). However, it was unascertained that the detected adult fulmars in 2019 were whether same individuals in 2018 or not. 3D habitat models would provide a clue on nest site preferences associated with vegetation (Fisher 1966).

Since not only fulmars but also kittiwakes have been monitored with the count unit of AON, long-term monitoring on the nest site would be useful in comprehending the breeding status. 3D habitat models would supply long-term data on the nest site carrying low and high breeding success in regard of topographical features. Several factors such as density, roof, and ledge were suggested to affect the breeding success in that kittiwakes select nest sites to protect the predators (Massaro et al. 2001; Regehr et al. 1998).

Chapter 6. Conclusions

RPAS-based monitoring is a growing field on conservation biology, and ethical issues regarding disturbance on wildlife has also dealt. In this study, RPAS was deployed in Svalbard coastal cliffs to survey colonial cliff-nesting seabirds such as kittiwakes and fulmars, obeying the guidelines and regulations of aviation safety. Kittiwakes showed minimal vigilance on the aircraft compared to the response of predators, but it should not be hastily concluded that RPAS did not make any immediate or continuous impact on physiological changes.

A total of 35 flights were completed, and thousands of images were obtained. RPAS-driven RGB images (4800x3200) taken within 50m from colonies were clear enough to distinguish every species. These images were used to construct fine-spatial 3D habitat models of each study through SfM photogrammetry. On the other hand, RPAS-driven thermal images (640x512) were much lower in resolution than RGB images, so the aircraft should approach coastal cliffs closer to obtain interpretable thermal images. For this reason, it was difficult to draw a reliable count only with use of thermal images. Thermal cameras still could be used to help the detection of cryptic seabirds and the semi-automated counts.

3D habitat models enabled it simple to calculate and compare densities among colonies. I developed the python script to count each neighbor modified from Massaro et al. (2001), and this method provided quantitative way to understand the relationship between the density and colony size. Application on other species is also promising.

Finally, long-term nest site monitoring would be suggested from a fulmar case study. This fulmar colony was small enough to determine the exact nest site one by one, and fulmars showed high nest site preferences. However, unless fulmars were marked individually, occupations of same nest sites by same pairs could not be guaranteed. If individual identification data existed, RPAS would go further and provide a simple platform to imply nest site fidelity.

References

- Aebischer, N., and J. Coulson (1990). Survival of the kittiwake in relation to sex, year, breeding experience and position in the colony. *The Journal of Animal Ecology*:1063-1071.
- Anderson, K., and K. J. Gaston (2013). Lightweight unmanned aerial vehicles will revolutionize spatial ecology. *Front Ecol Environ* 11:138-146.
- Anker-Nilssen, T., R. Barrett, B. Moe, T. K. Reiertsen, G. H. Systad, J. O. Bustnes, S. Christensen-Dalsgaard, S. Descamps, K.-E. Erikstad, A. Follestad, S. A. Hanssen, et al. (2019). Key-site monitoring in Norway 2018, including Svalbard and Jan Mayen. SEAPOP Short Report 1-2019:15.
- Anker-Nilssen, T., R. T. Barrett, J. O. Bustnes, S. Christensen-Dalsgaard, K. E. Erikstad, P. Fauchald, S.-H. Lorentsen, H. Steen, H. Strøm, and G. H. Systad (2008). SEAPOP studies in the Barents and Norwegian Seas in 2007. NINA rapport.
- Ashmole, N. (1962). The Black Noddy *Anous tenuirostris* on Ascension Island. Part 1. General biology. *Ibis* 103:235-273.
- Bakken, V. (1986). A method for assessing changes in the breeding population of guillemots *Uria aalge* on Vedøey, Roest. *Fauna Norvegica, Series C* 9:25-34.
- Barrett, R. T., S.-H. Lorentsen, and T. Anker-Nilssen (2006). The status of breeding seabirds in mainland Norway. *Atlantic Seabirds* 8:97-126.
- Bird, E. C. (1994). Cliff hazards and coastal management. *Journal of Coastal Research*:299-309.
- Birkhead, T. (1978). Attendance patterns of guillemots *Uria aalge* at breeding colonies on Skomer Island. *Ibis* 120:219-229.
- Birkhead, T., and D. Nettleship (1985). *The Atlantic Alcidae*. London: Academic Press Inc.
- Birkhead, T. R. (1977). The effect of habitat and density on breeding success in the common guillemot (*Uria aalge*). *The Journal of Animal Ecology*:751-764.
- Birkhead, T. R., and D. N. Nettleship (1980). Census methods for murrelets, *Uria* species: a unified approach. Canadian Wildlife Service.
- Brown, C. R., B. J. Stutchbury, and P. D. Walsh (1990). Choice of colony size in birds. *Trends in Ecology & Evolution* 5:398-403.
- Buckland, S. T., S. J. Marsden, and R. E. Green (2008). Estimating bird abundance: making methods work. *Bird Conservation International* 18:S91-S108.
- Burke, C., M. Rashman, S. Wich, A. Symons, C. Theron, and S. Longmore (2019). Optimizing observing strategies for monitoring animals using drone-mounted thermal infrared cameras. *International Journal of Remote Sensing* 40:439-467.

- Burns, J., D. Delparte, R. Gates, and M. Takabayashi (2015). Integrating structure-from-motion photogrammetry with geospatial software as a novel technique for quantifying 3D ecological characteristics of coral reefs. *PeerJ* 3:e1077.
- Cairns, D. (1988). Seabirds as indicators of marine food supplies. *Biological oceanography* 5:261-271.
- Chabot, D., and D. M. Bird (2012). Evaluation of an off-the-shelf unmanned aircraft system for surveying flocks of geese. *Waterbirds* 35:170-174.
- Chabot, D., S. Craik, and D. M. Bird (2015). Population census of a large Common Tern colony with a small unmanned aircraft. *PLoS One* 10:e0122588.
- Coulson, J., and J. M. Horobin (1972). The annual re-occupation of breeding sites by the Fulmar. *Ibis* 114:30-42.
- Coulson, J. C. (2002). Colonial breeding in seabirds. *Biology of marine birds*:87-113.
- Cullen, E. (1957). Adaptations in the Kittiwake to cliff-nesting. *Ibis* 99:275-302.
- Cullen, J., and N. Ashmole (1963). The Black Noddy *Anous tenuirostris* on Ascension Island. Part 2. Behaviour. *Ibis* 103:423-446.
- Dahl, T., S. Falk-Petersen, G. Gabrielsen, J. Sargent, H. Hop, and R. Millar (2003). Lipids and stable isotopes in common eider, black-legged kittiwake and northern fulmar: a trophic study from an Arctic fjord. *Marine Ecology Progress Series* 256:257-269.
- Danchin, E., and J. Nelson (1991). Behavioral adaptations to cliff nesting in the kittiwake (*Rissa tridactyla*): convergences with the gannet (*Sula bassana*) and the black noddy (*Anous tenuirostris*). *Colonial Waterbirds*:103-107.
- Danchin, E., and R. H. Wagner (1997). The evolution of coloniality: the emergence of new perspectives. *Trends in Ecology & Evolution* 12:342-347.
- Darling, F. F. (1938). Bird flocks and the breeding cycle; a contribution to the study of avian sociality.
- Ditmer, Mark A., John B. Vincent, Leland K. Werden, Jessie C. Tanner, Timothy G. Laske, Paul A. Iaizzo, David L. Garshelis, and John R. Fieberg (2015). Bears show a physiological but limited behavioral response to unmanned aerial vehicles. *Curr Biol* 25:2278-2283.
- Fang, Y.-T., M.-N. Tuanmu, and C.-M. Hung (2018). Asynchronous evolution of interdependent nest characters across the avian phylogeny. *Nature communications* 9:1-8.
- Fazio, N., M. Perrotti, G. Andriani, F. Mancini, P. Rossi, C. Castagnetti, and P. Lollino (2019). A new methodological approach to assess the stability of discontinuous rocky cliffs using in-situ surveys supported by UAV-based techniques and 3-D finite element model: a case study. *Engineering Geology* 260:105205.
- Fisher, J. (1952). The fulmar. HarperCollins.
- Fisher, J. (1966). The fulmar population of Britain and Ireland, 1959. *Bird Study* 13:5-76.

- Forsmoor, J., K. Anderson, C. J. Macleod, M. E. Wilkinson, L. DeBell, and R. E. Brazier (2019). Structure from motion photogrammetry in ecology: Does the choice of software matter? *Ecology and Evolution* 9:12964-12979.
- Gade, R., and T. B. Moeslund (2014). Thermal cameras and applications: a survey. *Machine vision and applications* 25:245-262.
- Gilchrist, H. G., and A. J. Gaston (1997). Effects of murre nest site characteristics and wind conditions on predation by glaucous gulls. *Canadian Journal of Zoology* 75:518-524.
- Goebel, M., W. Perryman, J. Hinke, D. Krause, N. Hann, S. Gardner, and D. LeRoi (2015). A small unmanned aerial system for estimating abundance and size of Antarctic predators. *Polar Biol* 38:619-630.
- Gonzalez, L., G. Montes, E. Puig, S. Johnson, K. Mengersen, and K. Gaston (2016). Unmanned aerial vehicles (UAVs) and artificial intelligence revolutionizing wildlife monitoring and conservation. *Sensors* 16:97.
- Hailman, J. P. (1964). Breeding synchrony in the equatorial Swallow-tailed Gull. *The American Naturalist* 98:79-83.
- Hailman, J. P. (1965). Cliff-nesting adaptations of the Galapagos swallow-tailed gull. *The Wilson Bulletin*:346-362.
- Harris, M. (1989). Variation in the correction factor used for converting counts of individual Guillemots *Uria aalge* into breeding pairs. *Ibis* 131:85-93.
- Harris, M., S. Wanless, T. Barton, and D. Elston (1997). Nest site characteristics, duration of use and breeding success in the guillemot *Uria aalge*. *Ibis* 139:468-476.
- Harris, M. P., M. Heubeck, M. A. Newell, and S. Wanless (2015). The need for year-specific correction factors (k values) when converting counts of individual Common Guillemots *Uria aalge* to breeding pairs. *Bird Study* 62:276-279.
- Hobson, K. A., and A. L. Bond (2012). Extending an indicator: year-round information on seabird trophic ecology from multiple-tissue stable-isotope analyses. *Marine Ecology Progress Series* 461:233-243.
- Hodgson, J. C., S. M. Baylis, R. Mott, A. Herrod, and R. H. Clarke (2016). Precision wildlife monitoring using unmanned aerial vehicles. *Scientific reports* 6:1-7.
- Hodgson, J. C., and L. P. Koh (2016). Best practice for minimising unmanned aerial vehicle disturbance to wildlife in biological field research. *Current Biology* 26:R404-R405.
- Hodgson, J. C., R. Mott, S. M. Baylis, T. T. Pham, S. Wotherspoon, A. D. Kilpatrick, R. Raja Segaran, I. Reid, A. Terauds, and L. P. Koh (2018). Drones count wildlife more accurately and precisely than humans. *Methods Ecol Evol* 9:1160-1167.
- Hop, H., T. Pearson, E. N. Hegseth, K. M. Kovacs, C. Wiencke, S. Kwasniewski, K. Eiane, F. Mehlum, B. Gulliksen, and M. Wlodarska-Kowalczyk (2002). The marine ecosystem of Kongsfjorden, Svalbard. *Polar Research* 21:167-208.

- Hunter, J. D. (2007). Matplotlib: A 2D graphics environment. *Computing in Science & Engineering* 9:90-95.
- Hutchinson, A. E. (1980). Estimating numbers of colonial nesting seabirds: a comparison of techniques. Pages 235-244 in *Proceedings of the Colonial Waterbird Group*, vol. 3. JSTOR.
- Israel, M., and A. Reinhard (2017). Detecting nests of lapwing birds with the aid of a small unmanned aerial vehicle with thermal camera. Pages 1199-1207 in *Unmanned Aircraft Systems (ICUAS), 2017 International Conference on*. IEEE.
- Iverson, S. J., A. M. Springer, and A. S. Kitaysky (2007). Seabirds as indicators of food web structure and ecosystem variability: qualitative and quantitative diet analyses using fatty acids. *Marine Ecology Progress Series* 352:235-244.
- Jaspers, V. L. B., S. Voorspoels, A. Covaci, G. Lepoint, and M. Eens (2007). Evaluation of the usefulness of bird feathers as a non-destructive biomonitoring tool for organic pollutants: A comparative and meta-analytical approach. *Environment International* 33:328-337.
- Jaud, M., P. Letortu, C. Théry, P. Grandjean, S. Costa, O. Maquaire, R. Davidson, and N. Le Dantec (2019). UAV survey of a coastal cliff face–Selection of the best imaging angle. *Measurement* 139:10-20.
- Kellenberger, B., D. Marcos, and D. Tuia (2018). Detecting mammals in UAV images: Best practices to address a substantially imbalanced dataset with deep learning. *Remote Sens Environ* 216:139-153.
- Kildaw, S. D. (1998). Population status and patterns of distribution and productivity of kittiwakes on St. George Island, Alaska.
- Kildaw, S. D. (1999). Competitive displacement? An experimental assessment of nest site preferences of cliff-nesting gulls. *Ecology* 80:576-586.
- Klukowski, P., M. Augoff, M. Zięba, M. Drwał, A. Gonczarek, and M. J. Walczak (2018). NMRNet: a deep learning approach to automated peak picking of protein NMR spectra. *Bioinformatics* 34:2590-2597.
- Korczak-Abshire, M., A. Zmarz, M. Rodzewicz, M. Kycko, I. Karsznia, and K. Chwedorzewska (2019). Study of fauna population changes on Penguin Island and Turret Point Oasis (King George Island, Antarctica) using an unmanned aerial vehicle. *Polar Biol* 42:217-224.
- Lhoest, S., J. Linchant, S. Quevauvillers, C. Vermeulen, and P. Lejeune (2015). How many hippos (HOMHIP): algorithm for automatic counts of animals with infra-red thermal imagery from UAV. *International Archives of the Photogrammetry, Remote Sensing and Spatial Information Sciences* 40.

- Liguang, S., Z. Renbin, Y. Xuebin, L. Xiaodong, X. Zhouqing, and W. Yuhong (2004). A geochemical method for the reconstruction of the occupation history of a penguin colony in the maritime Antarctic. *Polar Biology* 27:670-678.
- Mackenzie, D. (2012a). A flapping of wings. American Association for the Advancement of Science.
- Mackenzie, D. (2012b). It's a Bird, It's a Plane, It's a... Spy? American Association for the Advancement of Science.
- Mallory, M. L. (2008). Marine plastic debris in northern fulmars from the Canadian high Arctic. *Marine Pollution Bulletin* 56:1501-1504.
- Mallory, M. L., H. G. Gilchrist, B. M. Braune, and A. J. Gaston (2006). Marine birds as indicators of Arctic marine ecosystem health: linking the Northern Ecosystem Initiative to long-term studies. *Environmental Monitoring and Assessment* 113:31-48.
- Massaro, M., J. W. Chardine, and I. L. Jones (2001). Relationships between black-legged kittiwake nest-site characteristics and susceptibility to predation by large gulls. *The Condor* 103:793-801.
- McCafferty, D. J. (2013). Applications of thermal imaging in avian science. *Ibis* 155:4-15.
- Morrison, M. L. (1994). Resource inventory and monitoring: concepts and applications for ecological restoration. *Restoration & Management Notes* 12:179-183.
- Nelson, J. (1965). The behaviour of the Gannet. *Br. Birds* 58:233-288.
- Oliphant, T. E. (2007). Python for scientific computing. *Computing in Science & Engineering* 9:10-20.
- Ratcliffe, N., D. Guihen, J. Robst, S. Crofts, A. Stanworth, and P. Enderlein (2015). A protocol for the aerial survey of penguin colonies using UAVs (unmanned aerial vehicles). *J Unmanned Veh Sys* 3:95.
- Regehr, H. M., M. S. Rodway, and W. A. Montevecchi (1998). Antipredator benefits of nest-site selection in Black-legged Kittiwakes. *Canadian Journal of Zoology* 76:910-915.
- Rowan, M. (1952). The Greater Shearwater *Puffinus gravis* at its breeding grounds. *Ibis* 94:97-121.
- Rush, G. P., L. E. Clarke, M. Stone, and M. J. Wood (2018). Can drones count gulls? Minimal disturbance and semiautomated image processing with an unmanned aerial vehicle for colony-nesting seabirds. *Ecol Evol* 8:12322-12334.
- Sardà-Palomera, F., G. Bota, C. Viñolo, O. Pallarés, V. Sazatornil, L. Brotons, S. Gomáriz, and F. Sardà (2012). Fine-scale bird monitoring from light unmanned aircraft systems. *Ibis* 154:177-183.
- Scholten, C., A. Kamphuis, K. Vredevoogd, K. Lee-Strydhorst, J. Atma, C. Shea, O. Lamberg, and D. Proppe (2019). Real-time thermal imagery from an unmanned aerial vehicle

- can locate ground nests of a grassland songbird at rates similar to traditional methods. *J Biological Conservation* 233:241-246.
- Seabold, S., and J. Perktold (2010). *Statsmodels: Econometric and statistical modeling with python*. Page 61 in *Proceedings of the 9th Python in Science Conference*, vol. 57. Austin, TX.
- Shao, W., R. Kawakami, R. Yoshihashi, S. You, H. Kawase, and T. Naemura (2020). Cattle detection and counting in UAV images based on convolutional neural networks. *International Journal of Remote Sensing* 41:31-52.
- Squibb, R. C., and G. L. Hunt Jr (1983). A Comparison of Nesting-Ledges Used by Seabirds on St. George Island. *Ecology* 64:727-734.
- Ventura, D., A. Bonifazi, M. F. Gravina, A. Belluscio, and G. Ardizzone (2018). Mapping and classification of ecologically sensitive marine habitats using unmanned aerial vehicle (UAV) imagery and object-based image analysis (OBIA). *Remote Sensing* 10:1331.
- Vihtakari, M., J. Welcker, B. Moe, O. Chastel, S. Tartu, H. Hop, C. Bech, S. Descamps, and G. W. Gabrielsen (2018). Black-legged kittiwakes as messengers of Atlantification in the Arctic. *Scientific reports* 8:1-11.
- Virtanen, P., R. Gommers, T. E. Oliphant, M. Haberland, T. Reddy, D. Cournapeau, E. Burovski, P. Peterson, W. Weckesser, and J. Bright (2020). *SciPy 1.0: fundamental algorithms for scientific computing in Python*. *Nature methods* 17:261-272.
- Weissensteiner, M. H., J. W. Poelstra, and J. B. W. Wolf (2015). Low-budget ready-to-fly unmanned aerial vehicles: an effective tool for evaluating the nesting status of canopy-breeding bird species. *J Avian Biol* 46:425-430.
- Wheatley, D., and M. Gillings (2000). Vision, perception and GIS: developing enriched approaches to the study of archaeological visibility. *Nato Asi Series a Life Sciences* 321:1-27.
- Wickham, H. (2011). *ggplot2*. *Wiley Interdisciplinary Reviews: Computational Statistics* 3:180-185.
- Yuan, L., L. Sun, N. Long, Z. Xie, Y. Wang, and X. Liu (2010). Seabirds colonized Ny-Ålesund, Svalbard, Arctic~ 9,400 years ago. *Polar Biology* 33:683-691.

Appendix

Appendix 1

List of the detailed last observation records of seabird during summer seasons near Ny-Ålesund (modified form SEAPOP data portal)

Location	Observed date	Common name	Scientific name	Counts	Count unit
Blomstrandhalvøya SW	15.07.2011	Northern Fulmar	<i>Fulmarus glacialis</i>	32	AON
Blomstrandhalvøya SW	15.07.1973	Black Guillemot	<i>Cepphus grylle</i>	7	Pair
Blomstrandhamna 1	23.06.2011	Black-legged Kittiwake	<i>Rissa tridactyla</i>	908	AON
Blomstrandhamna 1	23.06.2011	Thick-billed Murre	<i>Uria lomvia</i>	239	Individual
Blomstrandhamna 1	23.06.2011	Northern Fulmar	<i>Fulmarus glacialis</i>	10	AON
Blomstrandhamna 1	23.06.2011	Atlantic Puffin	<i>Fratercula arctica</i>	5	Individual
Blomstrandhamna 1	23.06.2011	Barnacle Goose	<i>Branta leucopsis</i>	2	Pair
Blomstrandhamna 1	23.06.2011	Glaucous Gull	<i>Larus hyperboreus</i>	1	Pair
Blomstrandhamna 1	02.08.1981	Black Guillemot	<i>Cepphus grylle</i>	1	Individual
Blomstrandhamna 2	05.07.1973	Atlantic Puffin	<i>Fratercula arctica</i>	50	Individual
Blomstrandhamna 2	05.07.1973	Black Guillemot	<i>Cepphus grylle</i>	20	Pair
Blomstrandhamna 3	24.07.1981	Black-legged Kittiwake	<i>Rissa tridactyla</i>	194	Pair
Blomstrandhamna 3	24.07.1981	Northern Fulmar	<i>Fulmarus glacialis</i>	50	AON
Blomstrandhamna 3	05.07.1973	Thick-billed Murre	<i>Uria lomvia</i>	3	Individual
Blomstrandhamna Bird Sanct.	05.07.1993	Common Eider	<i>Somateria mollissima</i>	692	Pair
Blomstrandhamna Bird Sanct.	05.07.1993	Barnacle Goose	<i>Branta leucopsis</i>	32	Pair
Blomstrandhamna Bird Sanct.	05.07.1993	Glaucous Gull	<i>Larus hyperboreus</i>	3	Pair
Blomstrandhamna Bird Sanct.	19.06.1983	Pink-footed Goose	<i>Anser brachyrhynchus</i>	1	Pair
Brøggerfjellet S	21.07.1973	Atlantic Puffin	<i>Fratercula arctica</i>	300	Individual
Brøggerfjellet S	21.07.1973	Black-legged Kittiwake	<i>Rissa tridactyla</i>	10	Pair
Dietrichholmen	06.07.1993	Common Eider	<i>Somateria mollissima</i>	13	Pair
Eskjeret	03.07.1993	Common Eider	<i>Somateria mollissima</i>	772	Pair

Eskjeret	03.07.1993	Barnacle Goose	<i>Branta leucopsis</i>	19	Pair
Eskjeret	03.07.1993	Great Black-backed Gull	<i>Larus marinus</i>	1	Pair
Gorillaheimen	06.07.1981	Black Guillemot	<i>Cepphus grylle</i>	4	Pair
Gorillaheimen	08.06.1981	Glaucous Gull	<i>Larus hyperboreus</i>	3	Individual
Hansneset	09.07.1985	Black-legged Kittiwake	<i>Rissa tridactyla</i>	151	Pair
Hansneset	09.07.1985	Northern Fulmar	<i>Fulmarus glacialis</i>	31	AON
Hansneset	09.07.1985	Little Auk	<i>Alle alle</i>	25	Individual
Kiærstrand/Kiærfjellet	21.07.1973	Northern Fulmar	<i>Fulmarus glacialis</i>	700	AON
Kiærstrand/Kiærfjellet	15.07.1983	Atlantic Puffin	<i>Fratercula arctica</i>	400	Pair
Kiærstrand/Kiærfjellet	15.07.1983	Black-legged Kittiwake	<i>Rissa tridactyla</i>	10	Pair
Kongsfjorden fuglereservat	19.06.1983	Pink-footed Goose	<i>Anser brachyrhynchus</i>	15	Pair
Kongsfjorden fuglereservat	19.06.1983	Barnacle Goose	<i>Branta leucopsis</i>	8	Pair
Kongsfjordneset	11.07.1985	Black-legged Kittiwake	<i>Rissa tridactyla</i>	10	Pair
Kongsfjordneset	11.07.1985	Atlantic Puffin	<i>Fratercula arctica</i>	5	Pair
Kongsfjordneset	11.07.1985	Black Guillemot	<i>Cepphus grylle</i>	1	Pair
Krykkjefjell/Franskleir	14.07.1992	Black-legged Kittiwake	<i>Rissa tridactyla</i>	652	Pair
Krykkjefjell/Franskleir	10.07.1985	Little Auk	<i>Alle alle</i>	354	Pair
Krykkjefjell/Franskleir	14.07.1992	Thick-billed Murre	<i>Uria lomvia</i>	80	Individual
Krykkjefjell/Franskleir	10.07.1985	Black Guillemot	<i>Cepphus grylle</i>	4	Pair
Krykkjefjell/Tyskleir	13.07.1992	Black-legged Kittiwake	<i>Rissa tridactyla</i>	154	Pair
Krykkjefjellet	15.07.2011	Thick-billed Murre	<i>Uria lomvia</i>	47	Individual
Krykkjefjellet	22.07.2010	Arctic Tern	<i>Sterna paradisaea</i>	18	Pair
Krykkjefjellet	22.07.2010	Common Eider	<i>Somateria mollissima</i>	6	Individual
Lovénøyane, Juttaholmen	05.07.1993	Common Eider	<i>Somateria mollissima</i>	112	Pair
Lovénøyane, Juttaholmen	05.07.1993	Barnacle Goose	<i>Branta leucopsis</i>	12	Pair
Lovénøyane, Midtholmen	05.07.1993	Common Eider	<i>Somateria mollissima</i>	3	Pair
Lovénøyane, Midtholmen	05.07.1993	Pink-footed Goose	<i>Anser brachyrhynchus</i>	2	Pair
Lovénøyane, Midtholmen	05.07.1993	Barnacle Goose	<i>Branta leucopsis</i>	2	Pair
Lovénøyane, Observasjonsholmen	13.07.1992	Black-legged Kittiwake	<i>Rissa tridactyla</i>	89	Pair
Lovénøyane, Observasjonsholmen	06.08.1985	Thick-billed Murre	<i>Uria lomvia</i>	8	Pair
Lovénøyane, Observasjonsholmen	05.07.1993	Common Eider	<i>Somateria mollissima</i>	7	Pair
Lovénøyane, Observasjonsholmen	22.07.1981	Black Guillemot	<i>Cepphus grylle</i>	2	Individual

Lovénøyane, Observasjonsholmen	22.07.1981	Glaucous Gull	<i>Larus hyperboreus</i>	1	Individual
Lovénøyane, Storholmen	04.07.1993	Common Eider	<i>Somateria mollissima</i>	2070	Pair
Lovénøyane, Storholmen	01.08.1995	Arctic Tern	<i>Sterna paradisaea</i>	600	Individual
Lovénøyane, Storholmen	04.07.1993	Barnacle Goose	<i>Branta leucopsis</i>	229	Pair
Mietheholmen	06.07.1993	Common Eider	<i>Somateria mollissima</i>	240	Pair
Mietheholmen	06.07.1993	Barnacle Goose	<i>Branta leucopsis</i>	11	Pair
Ny-Ålesund	07.07.1995	Arctic Tern	<i>Sterna paradisaea</i>	50	Individual
Ossian Sarsfjellet	18.07.2011	Black-legged Kittiwake	<i>Rissa tridactyla</i>	1936	AON
Ossian Sarsfjellet	18.07.2011	Thick-billed Murre	<i>Uria lomvia</i>	1358	Individual
Ossian Sarsfjellet	10.07.1985	Little Auk	<i>Alle alle</i>	100	Individual
Ossian Sarsfjellet	10.07.1985	Black Guillemot	<i>Cephus grylle</i>	10	Pair
Ossian Sarsfjellet	18.07.2011	Glaucous Gull	<i>Larus hyperboreus</i>	2	AON
Prins Heinrichøya	06.07.1993	Common Eider	<i>Somateria mollissima</i>	173	Pair
Prins Heinrichøya	06.07.1993	Barnacle Goose	<i>Branta leucopsis</i>	10	Pair
Stuphallet	15.07.2011	Northern Fulmar	<i>Fulmarus glacialis</i>	127	AON
Stuphallet	15.07.2011	Atlantic Puffin	<i>Fratercula arctica</i>	8	Individual
Stuphallet	11.07.1985	Little Auk	<i>Alle alle</i>	6	Individual
Stuphallet	15.07.2011	Glaucous Gull	<i>Larus hyperboreus</i>	2	Pair
Stuphallet	15.07.2011	Barnacle Goose	<i>Branta leucopsis</i>	1	Individual
Stuphallet	15.07.2011	Black Guillemot	<i>Cephus grylle</i>	1	Individual
Sørvågen	09.07.1985	Black-legged Kittiwake	<i>Rissa tridactyla</i>	450	Pair
Sørvågen	09.07.1985	Thick-billed Murre	<i>Uria lomvia</i>	110	Individual
Sørvågen	09.07.1985	Little Auk	<i>Alle alle</i>	100	Individual
Sørvågen	09.07.1985	Northern Fulmar	<i>Fulmarus glacialis</i>	16	AON
Sørvågen	09.07.1985	Atlantic Puffin	<i>Fratercula arctica</i>	5	Pair
Sørvågen	09.07.1985	Black Guillemot	<i>Cephus grylle</i>	3	Pair

* Note: The abbreviation "AON" means apparently occupied nest / nest site.

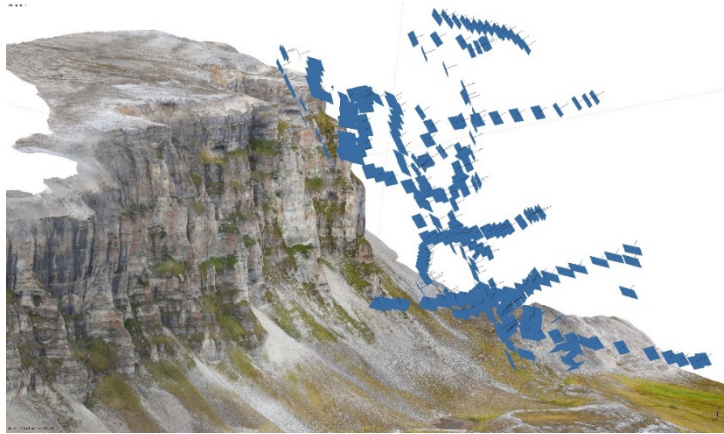
Appendix 2

Flight parameters and weather conditions

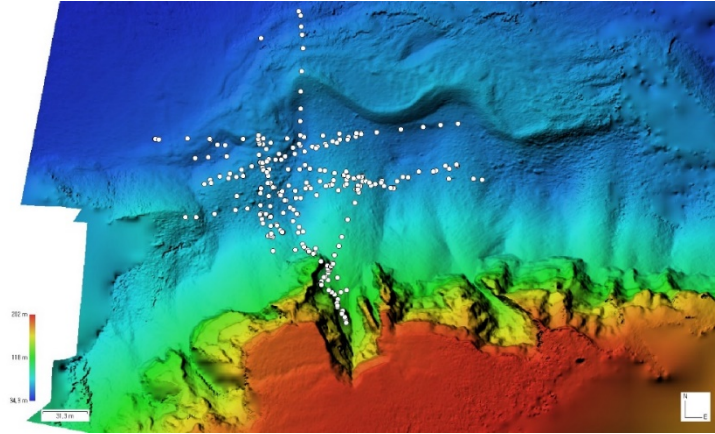
Area	Colony	Date	Take-off time	Flight duration (m)	Camera	Temperature (°C)	Wind speed (m/s)
Steinflåstupet		04.08.2018	18:27	3	RGB	9	1 – 2
			19:05	13	RGB		
Steinflåstupet		24.07.2019	15:22	10	RGB	11	3 – 4
Krykkjefjellet	Main	25.07.2019	14:33	7	RGB	10	2 – 3
	Main		14:51	14	RGB		
	Main		15:39	13	RGB		
Krykkjefjellet	Main	26.07.2019	12:44	8	Thermal	12	2 – 3
	Sub		14:18	5	RGB		
	Sub		15:13	12	Thermal		
Ossian Sarsfjellet	C D	27.07.2019	12:36	13	RGB	14	2 – 3
	C D		12:59	3	RGB		
Ossian Sarsfjellet	C D	29.07.2019	10:59	9	RGB	10	3 – 4
	C D		11:14	13	Both		
	C D		12:17	8	RGB		
Ossian Sarsfjellet	A B	30.07.2019	14:25	11	Both	10	2 – 3
	A B		14:42	11	Both		
Irgensfjellet	Left	30.07.2019	16:48	13	RGB	10	2 – 3
	Main		17:30	9	RGB		
	Main		17:46	11	RGB		
Kiærfjellet		31.07.2019	12:40	12	Both	10	2 – 3
			13:10	7	Both		
			13:44	9	Both		
Simlestupet		31.07.2019	14:49	15	Both	10	2 – 3
Irgensfjellet	Right	02.08.2019	10:42	4	Both	10	2 – 3
	Right		10:57	5	Both		
	Left		09:54	5	Both		

Steinflåstupet	Left	03.08.2019	10:08	6	Both	12	3 – 4
	Main		11:03	2	Both		
			13:31	8	Thermal		
			15:18	2	RGB		
Krykkjefjellet	Main	04.08.2019	14:10	7	Thermal	9	2 – 3
	Sub		14:25	5	Thermal		
	Main		15:12	6	RGB		
	Main		15:59	5	RGB		
	Sub		16:34	2	RGB		

Appendix 3-1



Captured view of the textured 3D model of Steinflåstupet and the locations of camera (blue rectangles)

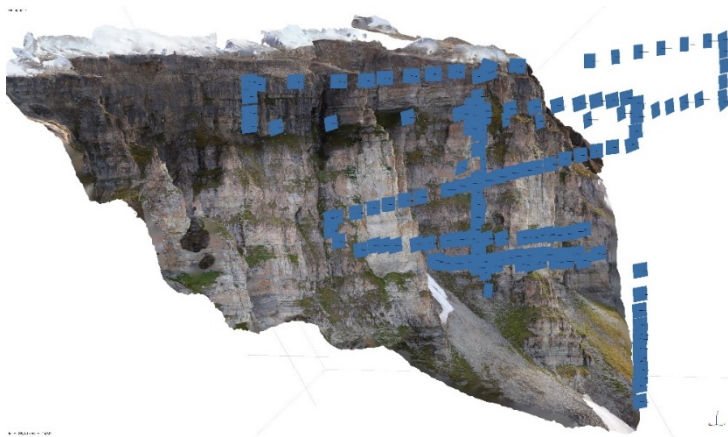


Captured view of the DEM with hillshading of Steinflåstupet and the locations of camera (white dots)

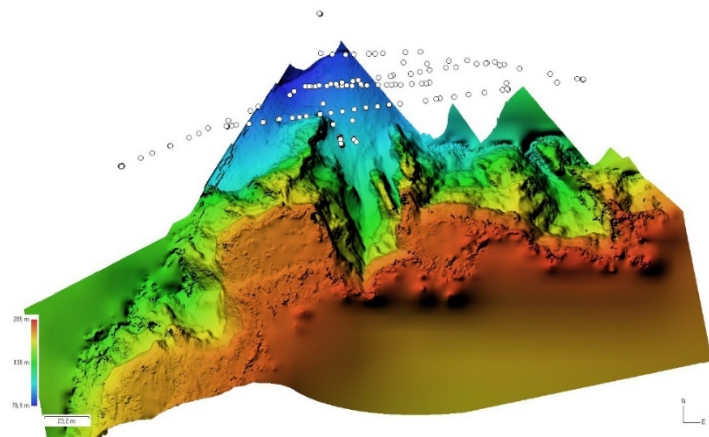
Detailed information of the above constructed models

Date	4 th August 2018
Camera details	SONY DSC-RX0 4800x3200
Used images	334/335 aligned
Dense cloud	23,978,381 points (medium quality)
Textured 3D model	1,594,431 faces (medium quality)
DEM	6,963x5,002, 9.9cm/pix (from dense cloud)

Appendix 3-2



Captured view of the textured 3D model of Steinflåstupet and the locations of camera (blue rectangles)

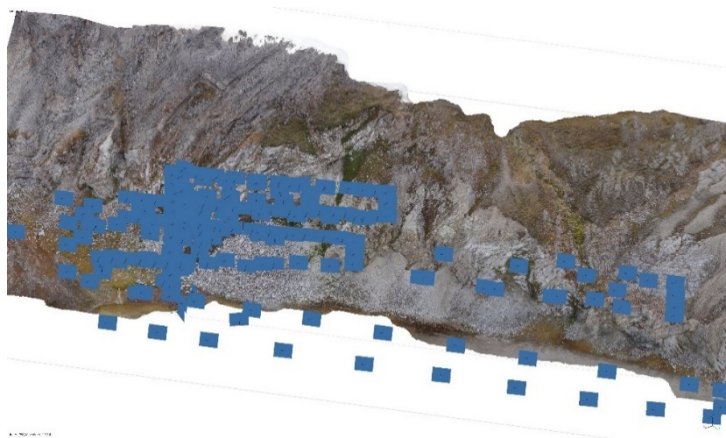


Captured view of the DEM with hillshading of Steinflåstupet and the locations of camera (white dots)

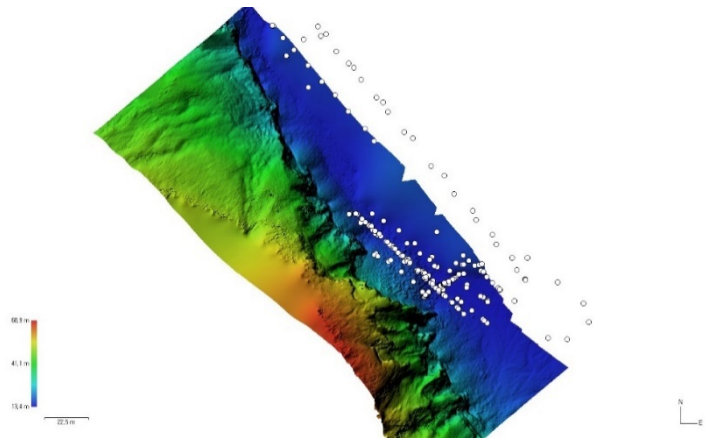
Detailed information of the above constructed models

Date	24 th July 2019
Camera details	SONY DSC-RX0 4800x3200
Used images	163/163 aligned
Dense cloud	3,684,596 points (low quality)
Textured model	226,471 faces (low quality)
DEM	3,031x2,310 (12.5cm/pix)

Appendix 3-3



Captured view of the textured 3D model of main colony in Krykkjefjellet and the locations of camera (blue rectangles)

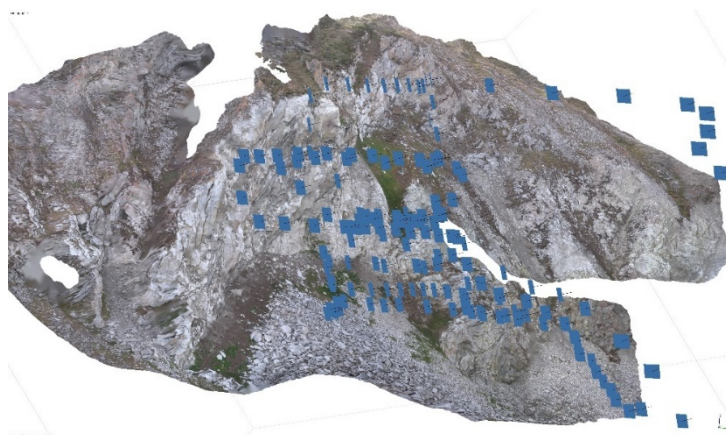


Captured view of the DEM with hillshading of main colony in Krykkjefjellet and the locations of camera (white dots)

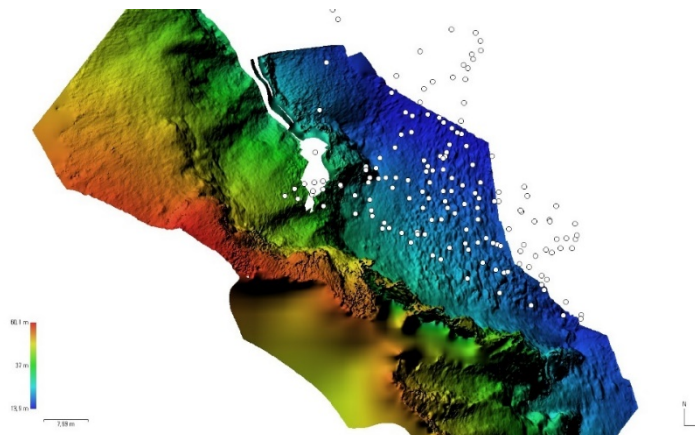
Detailed information of the above constructed models

Date	25th July 2019
Camera details	SONY DSC-RX0 4800x3200
Used images	208/208 aligned
Dense cloud	5,287,302 points (low quality)
Textured model	352,479 faces (low quality)
DEM	3,489x3,744 (7.06cm/pix)

Appendix 3-4



Captured view of the textured 3D model of main colony in Krykkjefjellet and the locations of camera (blue rectangles)

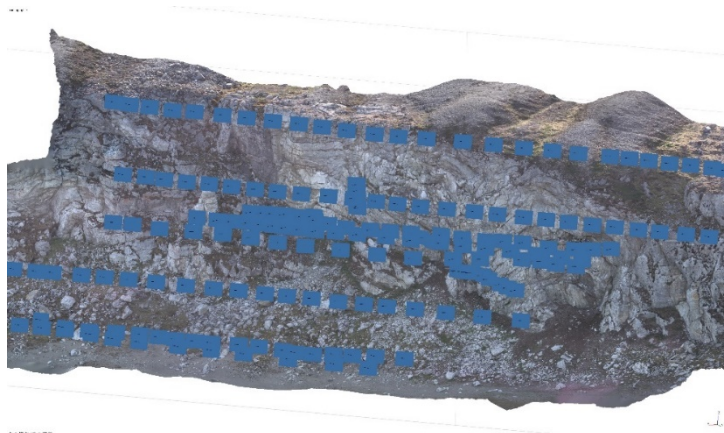


Captured view of the DEM with hillshading of main colony in Krykkjefjellet and the locations of camera (white dots)

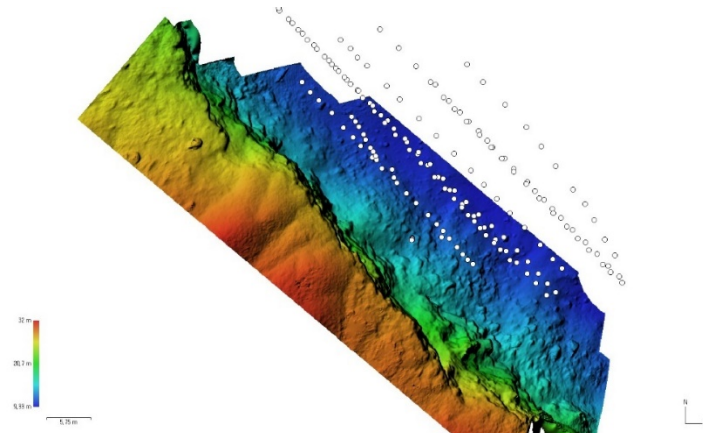
Detailed information of the above constructed models

Date	4 th August 2019
Camera details	SONY DSC-RX0 4800x3200
Used images	160/160 aligned
Dense cloud	4,480,810 points (low quality)
Textured model	298,709 faces (low quality)
DEM	3,071x3,070 (3.96cm/pix)

Appendix 3-5



Captured view of the textured 3D model of subcolony in Krykkjefjellet and the locations of camera (blue rectangles)

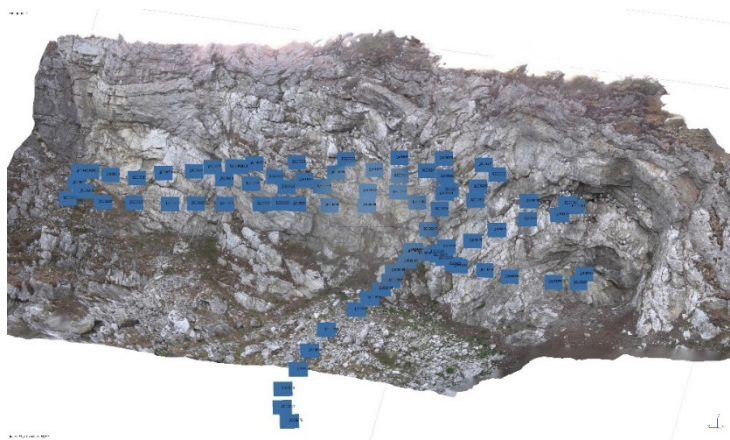


Captured view of the DEM with hillshading of subcolony in Krykkjefjellet and the locations of camera (white dots)

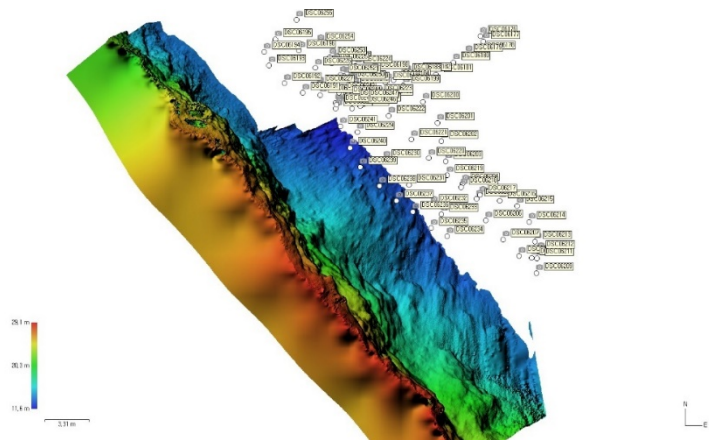
Detailed information of the above constructed models

Date	26 th July 2019
Camera details	SONY DSC-RX0M2 4800x3200
Used images	177/177 aligned
Dense cloud	2,847,449 points (low quality)
Textured model	569,457 faces (low quality)
DEM	2,362x2,173 (3.29cm/pix)

Appendix 3-6



Captured view of the textured 3D model of subcolony in Krykkjefjellet and the locations of camera (blue rectangles)

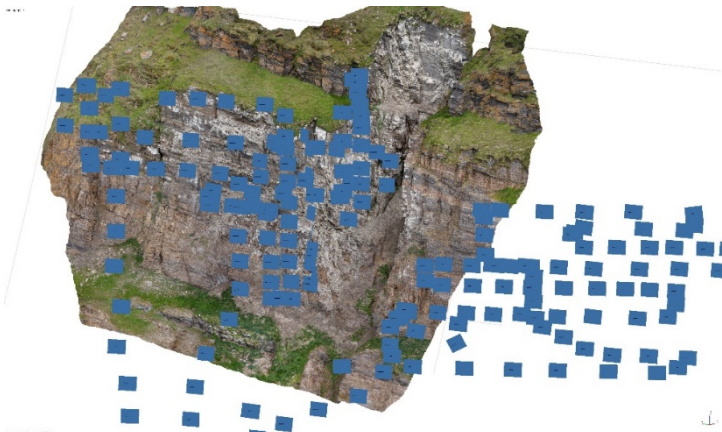


Captured view of the DEM with hillshading of subcolony in Krykkjefjellet and the locations of camera (white dots)

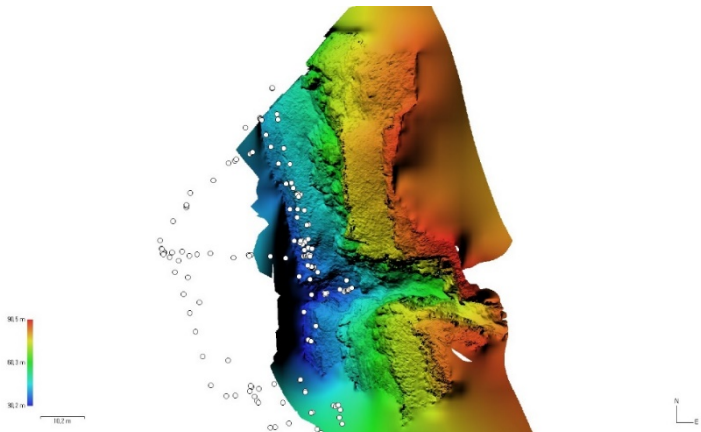
Detailed information of the above constructed models

Date	29 th July 2019
Camera details	SONY DSC-RX0 4800x3200
Used images	82/82 aligned
Dense cloud	8,060,970 points (medium quality)
Textured model	399,510 faces (medium quality)
DEM	1,767x4,149 (1.49cm/pix)

Appendix 3-7



Captured view of the textured 3D model of A subcolony in Ossian Sarsfjellet and the locations of camera (blue rectangles)

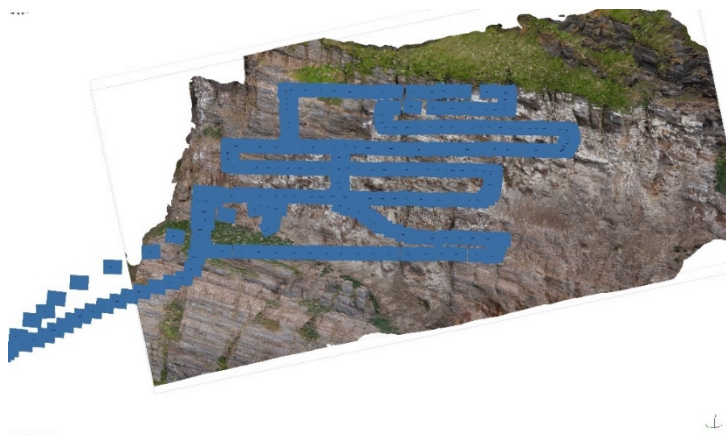


Captured view of the DEM with hillshading of A subcolony in Ossian Sarsfjellet and the locations of camera (white dots)

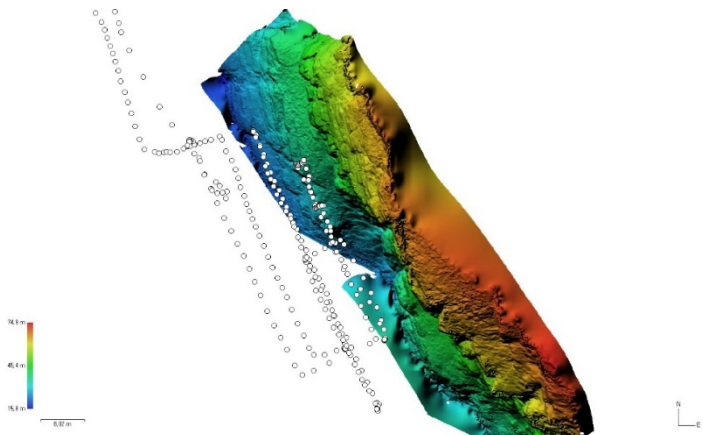
Detailed information of the above constructed models

Date	30 th July 2019
Camera details	SONY DSC-RX0 4800x3200
Used images	215/216 aligned
Dense cloud	19,076,938 points (medium quality)
Textured model	1,223,661 faces (medium quality)
DEM	5,914x7,934 (2.03cm/pix)

Appendix 3-8



Captured view of the textured 3D model of A subcolony in Ossian Sarsfjellet and the locations of camera (blue rectangles)

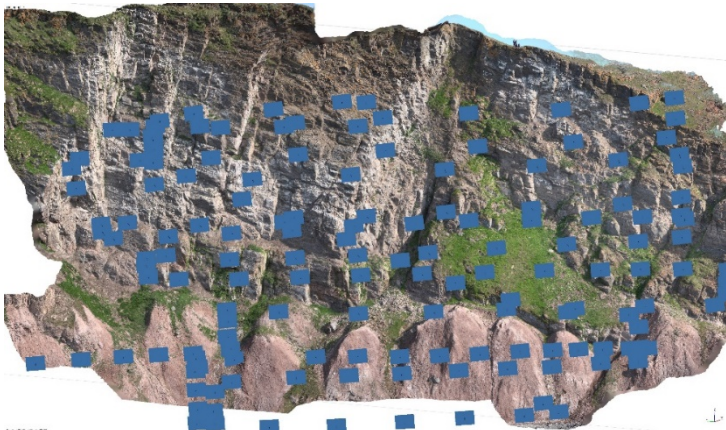


Captured view of the DEM with hillshading of A subcolony in Ossian Sarsfjellet and the locations of camera (white dots)

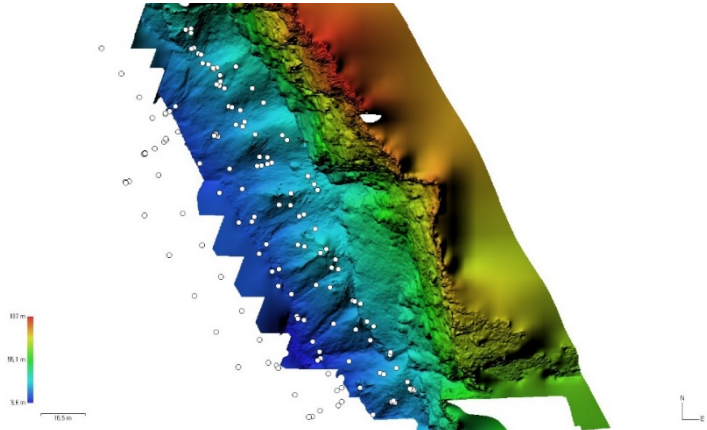
Detailed information of the above constructed models

Date	30 th July 2019
Camera details	SONY DSC-RX0 4800x3200
Used images	303/303 aligned
Dense cloud	15,805,681 points (medium quality)
Textured model	1,053,688 faces (medium quality)
DEM	3,635x5,125 (2.02cm/pix)

Appendix 3-9



Captured view of the textured 3D model of A subcolony in Ossian Sarsfjellet and the locations of camera (blue rectangles)

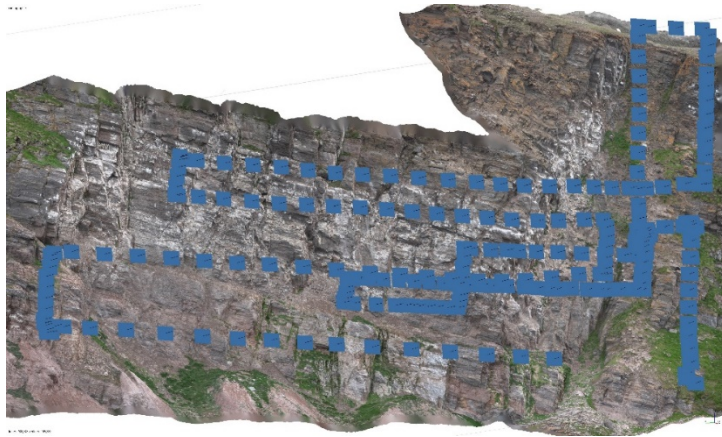


Captured view of the DEM with hillshading of A subcolony in Ossian Sarsfjellet and the locations of camera (white dots)

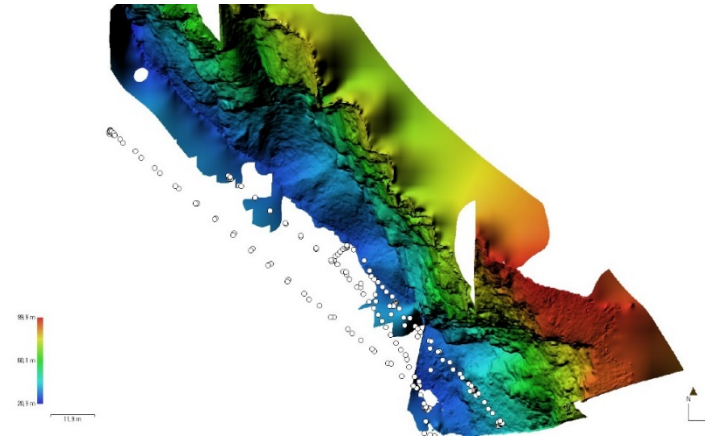
Detailed information of the above constructed models

Date	27 th July 2019
Camera details	SONY DSC-RX0M2 4800x3200
Used images	154/172 aligned
Dense cloud	6,048,274 points (low quality)
Textured model	130,310 faces (low quality)
DEM	3,328x4,089 (6.58cm/pix)

Appendix 3-10



Captured view of the textured 3D model of A subcolony in Ossian Sarsfjellet and the locations of camera (blue rectangles)

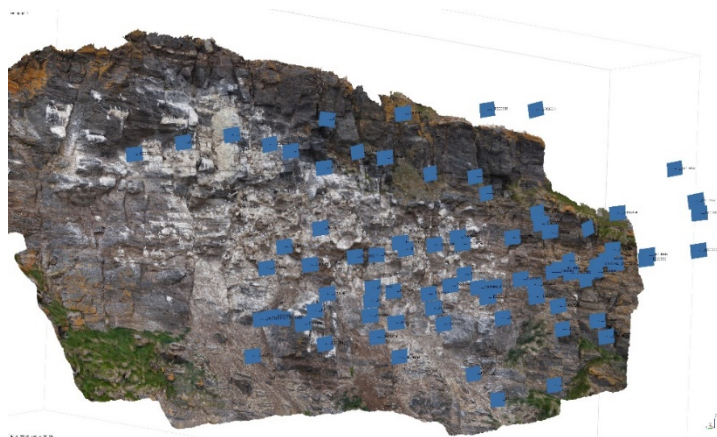


Captured view of the DEM with hillshading of A subcolony in Ossian Sarsfjellet and the locations of camera (white dots)

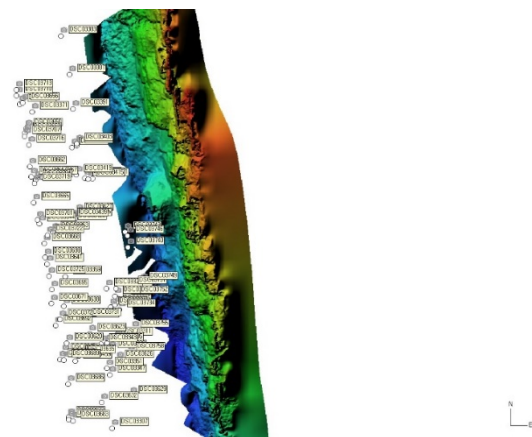
Detailed information of the above constructed models

Date	29 th July 2019
Camera details	SONY DSC-RX0M2 4800x3200
Used images	224/224 aligned
Dense cloud	4,947,515 points (low quality)
Textured model	328,648 faces (low quality)
DEM	3,106x3,376 (5.59cm/pix)

Appendix 3-11



Captured view of the textured 3D model of D subcolony in Ossian Sarsfjellet and the locations of camera (blue rectangles)

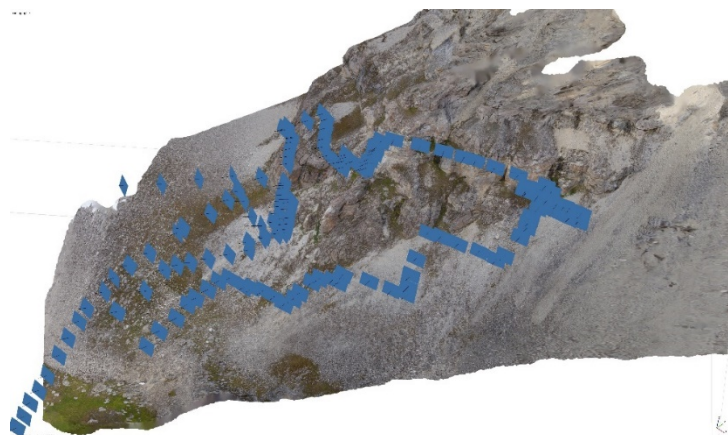


Captured view of the DEM with hillshading of D subcolony in Ossian Sarsfjellet and the locations of camera (white dots)

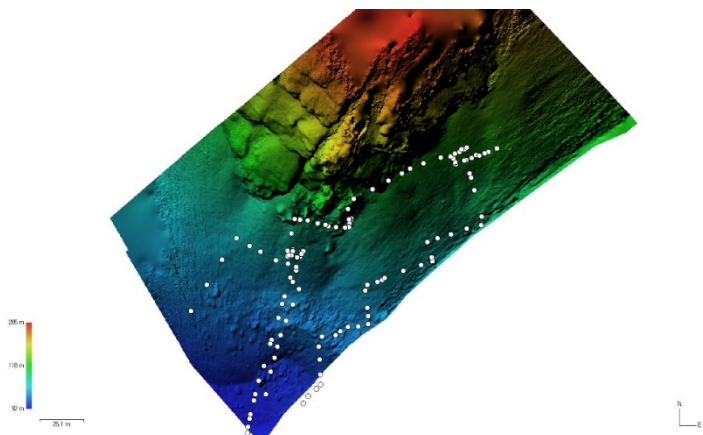
Detailed information of the above constructed models

Date	29 th July 2019
Camera details	SONY DSC-RX0 4800x3200
Used images	82/82 aligned
Dense cloud	8,060,970 points (medium quality)
Textured model	399,510 faces (medium quality)
DEM	1,767x4,149 (1.49cm/pix)

Appendix 3-12



Captured view of the textured 3D model of Kiærfjellet and the locations of camera (blue rectangles)

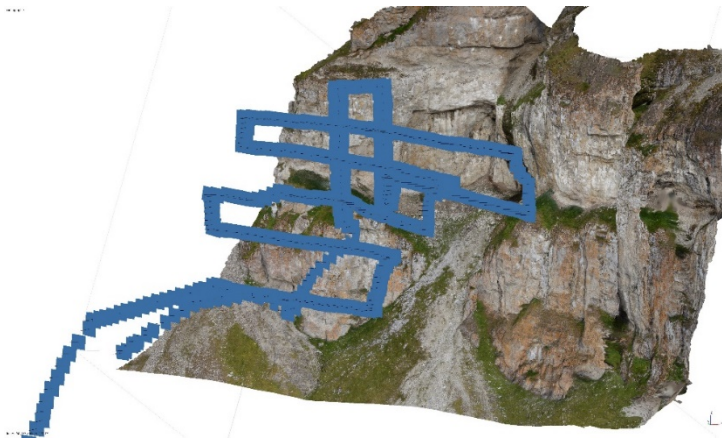


Captured view of the DEM with hillshading of Kiærfjellet and the locations of camera (white dots)

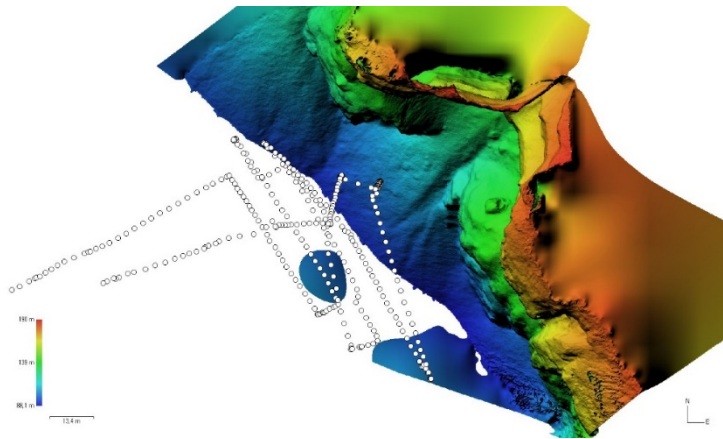
Detailed information of the above constructed models

Date	31 st July 2019
Camera details	SONY DSC-RX0 4800x3200
Used images	153/221 aligned
Dense cloud	3,521,207 points (low quality)
Textured model	234,513 faces (low quality)
DEM	2,710x2,615 (12.4cm/pix)

Appendix 3-13



Captured view of the textured 3D model of Simlestupet and the locations of camera (blue rectangles)

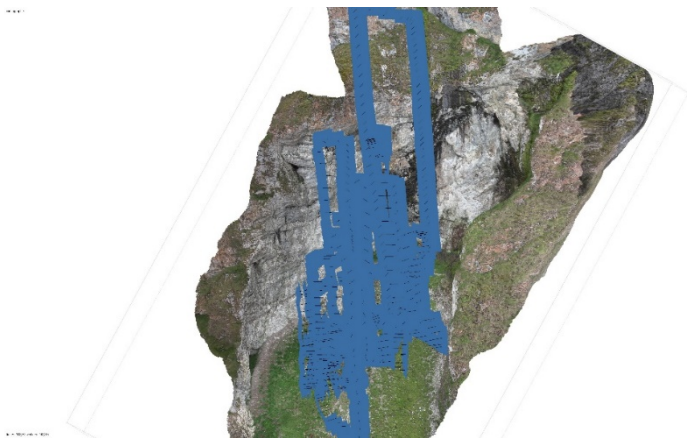


Captured view of the DEM with hillshading of Simlestupet and the locations of camera (white dots)

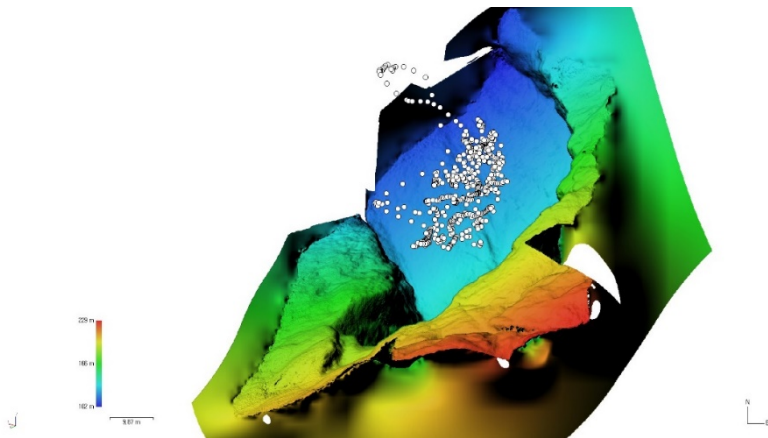
Detailed information of the above constructed models

Date	31 st July 2019
Camera details	SONY DSC-RX0 4800x3200
Used images	360/360 aligned
Dense cloud	1,810,573 points (medium quality)
Textured model	341,585 faces (medium quality)
DEM	1,610x1,763 (12cm/pix)

Appendix 3-14



Captured view of the textured 3D model of main colony in Irgensfjellet and the locations of camera (blue rectangles)

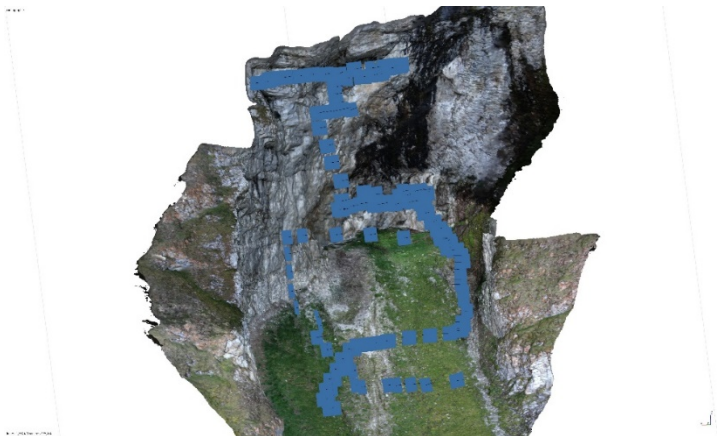


Captured view of the DEM with hillshading of main colony in Irgensfjellet and the locations of camera (white dots)

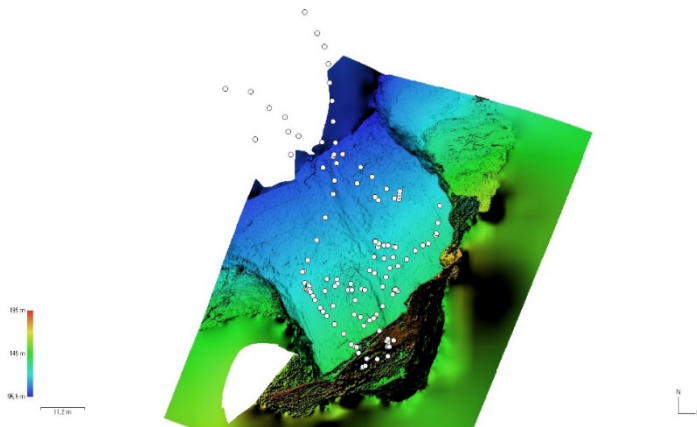
Detailed information of the above constructed models

Date	30 th July 2019
Camera details	SONY DSC-RX0M2 4800x3200
Used images	613/613 aligned
Dense cloud	1,683,395 points (lowest quality)
Textured model	322,682 faces (lowest quality)
DEM	1,419x1,657 (9.41cm/pix)

Appendix 3-15



Captured view of the textured 3D model of main colony in Irgensfjellet and the locations of camera (blue rectangles)

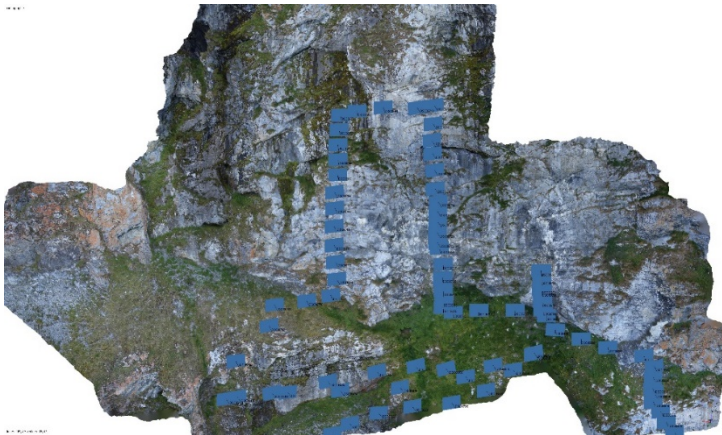


Captured view of the DEM with hillshading of main colony in Irgensfjellet and the locations of camera (white dots)

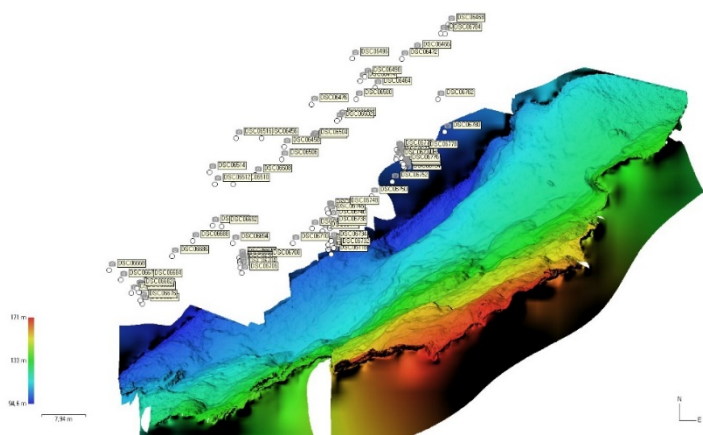
Detailed information of the above constructed models

Date	2 nd August 2019
Camera details	SONY DSC-RX0 4800x3200
Used images	128/128 aligned
Dense cloud	27,966,610 points (medium quality)
Textured model	1,864,429 faces (medium quality)
DEM	5,403x6,502 (2.14cm/pix)

Appendix 3-16



Captured view of the textured 3D model of right subcolony in Irgensfjellet and the locations of camera (blue rectangles)

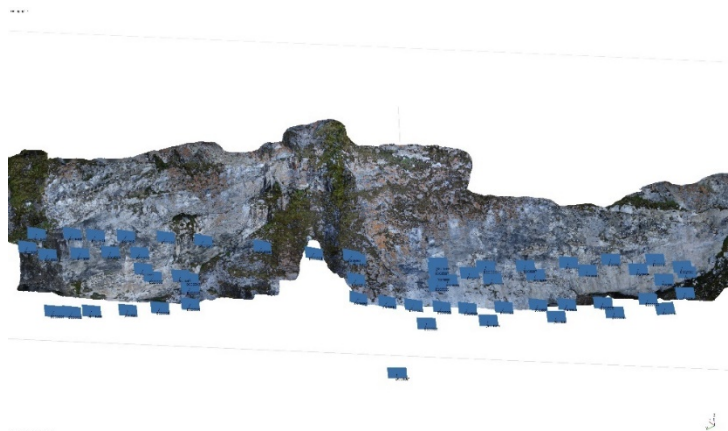


Captured view of the DEM with hillshading of right subcolony in Irgensfjellet and the locations of camera (white dots)

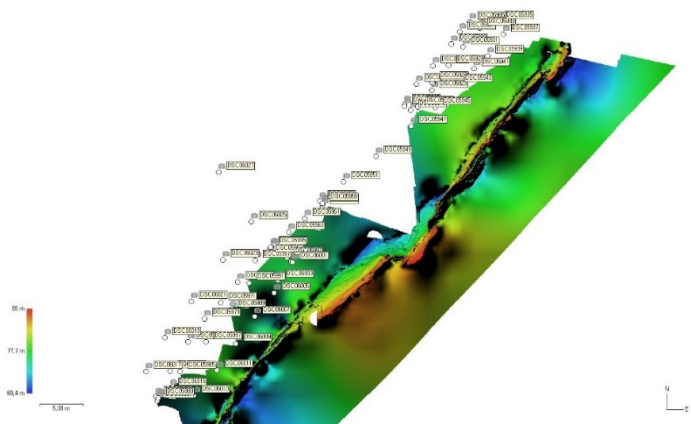
Detailed information of the above constructed models

Date	2 nd August 2019
Camera details	SONY DSC-RX0 4800x3200
Used images	81/88 aligned
Dense cloud	2,575,466 points (low quality)
Textured model	169,725 faces (low quality)
DEM	2,343x1,760 (5.61cm/pix)

Appendix 3-17



Captured view of the textured 3D model of left subcolony in Irgensfjellet and the locations of camera (blue rectangles)



Captured view of the DEM with hillshading of left subcolony in Irgensfjellet and the locations of camera (white dots)

Detailed information of the above constructed models

Date	2 nd August 2019
Camera details	SONY DSC-RX0 4800x3200
Used images	68/72 aligned
Dense cloud	17,609,928 points (medium quality)
Textured model	122,904 faces (medium quality)
DEM	6,993x7,503 (1.07cm/pix)

국문 초록

원격조종항공기시스템을 활용한 스발바르 해안절벽의 세가락갈매기 및 풀머갈매기에 대한 공간 분포 분석

정확한 개체수를 추정하고 개체군 변동을 이해하는 것은 보전생물학에서 매우 중요하다. 해양조류는 해양 생태계에서 매우 중요한 역할을 수행함에도 해안절벽에서 집단으로 번식하는 해양조류에 대해서는 낮은 접근성으로 인해 효과적인 모니터링이 어려웠다. 본 연구에서는 북극해에 둘러싸인 노르웨이의 스발바르 제도의 극한 환경에서 특히 세가락갈매기(*Rissa tridactyla*) 및 풀머갈매기 (*Fulmarus glacialis*)와 같이 해안절벽에서 집단 번식하는 해양조류의 조사를 위해 원격조종항공기시스템(RPAS, Remotely Piloted Aircraft System)을 활용하였다.

2018년과 2019년의 번식기 동안 RPAS로부터 해안절벽의 RGB (적·녹·청)와 열화상 사진을 획득하여 조사지역의 삼차원 모델을 구축하였다. 그리고 이 모델은 전체 해양조류의 개체수를 조사하고 세가락갈매기와 풀머갈매기의 공간 분포를 분석하는 데에 사용되었다. RPAS에 의해 얻어진 RGB와 열화상 사진으로 구성된 모델을 지상의 관찰자에 의해 촬영된 사진과 비교할 수 있었으며, 보이거나 숨겨진 지역이 지리정보시스템 소프트웨어의 가시권역 분석에 의해 결정되었다. 열화상 영상을 온도 값과 픽셀 크기에 따라 처리하였고, RGB 영상과 복합적으로 사용한 예시를 제시하였다. 성체 세가락갈매기의 0.8m 반경 이내의 개체수 평균으로 정의된 밀도를 계산하고 이 밀도와 개체군 크기의 관계에 대해 조사하였다. 또한 두 해 동안 같은 방법으로 조사된 Steinflåstupet 지역에서 비슷한 동지 위치를 점유하는지 알아보기 위해 풀머갈매기 새끼를 관찰하였다.

Irgensfjellet 개체군의 조사 결과는 지상 관찰자에 의해 촬영된 사진을 이어 붙인 것보다 RPAS에 의해 얻어진 RGB 영상 모델에서 평균 1.6배의 세가락갈매기가 탐지되었음을 보여주었다. 반면에 Irgensfjellet 보다 높은 비율의 가시 지역을 지녔던 Krykkjefjellet는 충분히 접근하여 관찰할 수 있던 지형이었기 때문에 영상 모델에 따른 개체수 조사 결과가 유의미하게 다르지 않았다. 또한 이 연구를 통해 RGB 영상과 관련하여 위장이 잘 된 해양조류를 발견하는 데에 열화상 사진이 상호보완적으로 사용될 수 있는 잠재력을 확인할 수 있었다. 추가적으로, 온도 값과 픽셀 크기의 범위를 적절히 조절하고 분류함으로써 해양조류의 반자동적 개체수 조사가 가능하였다. 성체 세가락갈매기의 밀도를 추정하기 위한 RPAS 자료는 전통적인 관찰이 오류를 범할 수 있으며, 삼차원 모델에서 계산된 세가락갈매기 밀도보다 과대추정될 수 있음을 보여주었다. 2019년에 발견된 일곱 마리의 풀머갈매기 새끼 모두 2018년에 이미 발견된 둥지 위치에 서식하는 것으로 보아 같은 둥지 위치가 두 해 이상 연속으로 점유된 것을 알 수 있었다.

결론적으로 RGB와 열화상 카메라가 함께 사용될 때, 절벽에 둥지를 짓는 해양조류의 모니터링에 RPAS가 중요한 도구로 작용하게 될 것이다. 절벽에서 번식하는 다른 해양조류 중에도 밀도와 공간 분포에 대한 분석을 확대하여 적용할 수 있다. 높은 둥지 위치 선호도를 보이는 풀머갈매기의 예시처럼 장기 모니터링의 관점에서 연간 둥지 위치의 변화가 RPAS에 의해 기록될 수 있을 것이다.

주요어: 원격조종항공기시스템, 스발바르 해양조류, 해안절벽, 절벽에서 둥지 짓기, 집단 번식, 세가락갈매기, 풀머갈매기

학번: 2018-21328